REVIEW ARTICLE

ABOUT

NUMERICAL METHODS IN HEAT TRANSFER RESEARCH

BY

Karam Mahmoud El-Shazly

Mechanical Eng. Dept., Shoubra Faculty of Eng.,
Zagazig University

October; 2000

CONTENTS

NUMERICAL METHODS IN HEAT TRANSFER RESEARCH

1. INTRODUCTION

The main objective of the paper is to convey methodology for the numerical solution of heat transfer and related fluid flow problems. The paper topics include finite-difference and finite-element methods for parabolic and elliptic systems; a comparative appraisal of finite-difference versus finite-element methods; Monte Carlo methods; finite analytic methods and average magnitude analysis method for supercomputers.

A detailed comparison of the finite-difference and finite-element methods in their classical forms is presented. Particular emphasis is on the evaluation and propagation of errors in both methods.

The relatively recent finite analytical method is used for one-, two-, and three-dimensional problems, including conduction heat transfer, natural and forced convection, and subsonic and supersonic flow problems. Mont Carlo method is used for solving conduction and convection problems as well as radiative transfer problems. Absorbing and emitting media are included. Methods for integral and integro-differential systems with particular attention given to the influence of radiative transfer are presented due to illustrative applications. Radiation, conduction-radiation, and conduction-convection-radiation problems are considered, including emitting, absorbing, and scattering media.

2. FINITE-DIFFRENCE METHODS FOR PARTIAL DIFFERENTIAL EQUATIONS

The basic techniques needed in the formulation of finite-difference representation are introduced. In the finite-difference approach, the problem domain is "discretized" so that the dependent variables are considered to exist only at discrete points. Derivatives are approximated by differences resulting in an algebraic representation of the partial differential equation(PDE). The nature of the resulting system of algebraic equations depends on the character of the problem posed by the original PDE (or system of PDEs). Partial differential equations in two independent variables can be classified as elliptic or parabolic. Each class has distinguishing features. The Laplace and poission equations, which govern many important physical processes, are examples of elliptic PDEs. More specificanlly, Laplace's equation goverms the steady-state temperature distribution in a homogeneous solid. The unsteady heat conduction(or "diffusion") equation is an example of a parabolic PDE. Elliptic PDEs are said to govern "equilibrium" problems, and parabolic equations govern "marching " problems.

Equilibrium problems occur on a closed domain, and the solution must meet prescribed conditions on all the boundaries. A single solution is sought that satisfies both the PDE and the boundary conditions. In contrast, marching problems arise on open domains - at least, the solution cannot be forced to meet specific conditions at more than one value of the timelike variable. Initial conditions must be specified for marching problems, but the other end of the time interval is open. The solution is "marched" in time from the initial conditions. For problems occuring in a region (physical space) of finite extent boundary conditions must be specified. For some

problems for which the extent of the region and boundary conditions must be specified. For some problems for which the extent of the region and boundary conditions are fixed, a time-asymptotic(steady) solution is approached at large values of the timelike variable.

Fundamental to finite-difference(and finite element) techniques is the concept of discretization: A physical domain is divided into a sequence of subdomains known as a nodal mesh, and approximations to a continuous solutions are defined at the nodal points.

Development of the approximations is generally done using either interpolating polynomials or Tayler series expansions. The Tayler series expansion is the most commonly used method since it provides error estimates. A discussion on the use of both interpolating polynomials and Tayler series expansion can be found in Pinder and Gray[1].

Suppose an approximation for the second derivative of a scalar quantity is developed using only the three nodal points i-1,i, and i+1. The use of Tayler series expansions allows the higher-order terms to term to be examined in order to ascertain the error of the approximation, which is not evident when using interpolating polynomials. Table. 1 lists the most commonly used difference expressions and their leading truncation terms, where the nth derivative of $\phi(x)$ and k,l are integers depending on n and the degree of accuracy of the approximation.

For physical problems, the term" boundary " literally means on the physical boundary of the region in a space which the solution is sought. The three most common boundary conditions are:

TABLE 1 Finite-Difference Discretizations

n	k	l	Derivative	Difference Expression	Truncation Error
1	1	1	$\frac{\partial \phi}{\partial x}$	$\frac{\phi_{i+1} - \phi_{i-1}}{2\Delta x}$	$\frac{(\Delta x)^2}{6}\frac{\partial^3 \phi}{\partial x^3} - \cdots$
1	1	1	$\frac{\partial \phi}{\partial x}$	$\frac{\phi_i - \phi_{i-1}}{\Delta x}$	$-\frac{\Delta x}{2}\frac{\partial^2 \phi}{\partial x^2} - \cdots$
1	1	1	$\frac{\partial \phi}{\partial x}$	$\frac{\phi_{i+1} - \phi_i}{\Delta x}$	$\frac{\Delta x}{2}\frac{\partial^2 \phi}{\partial x^2} - \cdots$
1	2	0	$\frac{\partial \phi}{\partial x}$	$\frac{3\phi_i - 4\phi_{i-1} + \phi_{i-2}}{2\Delta x}$	$-\frac{(\Delta x)^2}{3}\frac{\partial^3 \phi}{\partial x^3} - \cdots$
1	0	2	$\frac{\partial \phi}{\partial x}$	$\frac{-3\phi_i + 4\phi_{i+1} - \phi_{i+2}}{2\Delta x}$	$-\frac{(\Delta x)^2}{3}\frac{\partial^3 \phi}{\partial x^3} - \cdots$
1	2	2	$\frac{\partial \phi}{\partial x}$	$\frac{-\phi_{i+2} + 8\phi_{i+1} - 8\phi_{i-1} + \phi_{i-2}}{12\Delta x}$	$-\frac{(\Delta x)^4}{30}\frac{\partial^5 \phi}{\partial x^5} - \cdots$
2	1	1	$\frac{\partial^2 \phi}{\partial x^2}$	$\frac{\phi_{i-1} - 2\phi_i + \phi_{i-1}}{(\Delta x)^2}$	$\frac{(\Delta x)^2}{12}\frac{\partial^4 \phi}{\partial x^4} - \cdots$
2	2	2	$\frac{\partial^2 \phi}{\partial x^2}$	$\frac{-\phi_{i-2} + 16\phi_{i-1} - 30\phi_i + 16\phi_{i+1} - \phi_{i+2}}{12(\Delta x)^2}$	$\frac{(\Delta x)^4}{90}\frac{\partial^6 \phi}{\partial x^6} - \cdots$

(a) Value of dependent variable specified on the boundary. This boundary condition is also known as a Dirichlet condition or a boundary condition of the first kind.
(b) Normal derivative specified on the boundary. This condition is known as a Neumann condition or a boundary condition of the second kind.
© A linear combination of conditions (a) and (b), convective boundary conditions in heat transfer are of this type. This condition is known as a Robbins condition, a mixed condition, or a boundary condition of the third kind.

2-1 Difference Representation By Control Volume Analysis

One of the simplest PDEs having important physical applications is the parabolic one-dimensional heat diffusion equation

$$\frac{\partial T}{\partial t} = \alpha \frac{\partial^2 T}{\partial x^2} \tag{1}$$

In identifying the conservation principle represented by Eq. (1), it is helpful to represent the thermal diffusivity α as $\alpha = k/\rho C$, where k is the thermal conductivity, ρ the density and C the specific heat. These properties will be assumed to be constant in this example. The heat diffusion equation can be rearranged into the form

$$\rho C \frac{\partial T}{\partial t} = -\nabla q \tag{2}$$

where q is the heat flux vector, which is nearly $-k(\partial T/\partial x)$ for a one-dimensional problem. Choosing time level n for evaluation of the heat flow into the control volume gives

$$\rho C \frac{T_j^{n+1} - T_j^n}{\Delta t} \Delta x A = kA \left.\frac{\partial T}{\partial x}\right|_{j+\frac{1}{2}}^{n} - kA \left.\frac{\partial T}{\partial x}\right|_{j-\frac{1}{2}}^{n} \tag{3}$$

An internal control volume (left hand-side of Eq. (3)) will be considered using a forward difference in time $\rho C \frac{T_j^{n+1} - T_j^n}{\Delta t} \Delta x A$ where A is a unit area perpendicular to the x coordinate. While right hand-side of Eq. (3) is included using a central difference.

2-2 Simple Explicit Method

The simple explicit finite-difference representation of the heat equation (1) has been given as [2]

$$\frac{T_j^{n+1} - T_j^n}{\Delta t} = \alpha \frac{T_{j+1}^n - 2T_j^n + T_{j-1}^n}{(\Delta x)^2} \tag{4}$$

2-3 Simple Implicit Method

The simple implicit scheme for the heat diffusion equation can be developed from the Taylor series or control-volume methods by simply evaluating the heat diffusion term at the n+1 time level:

$$\frac{T_j^{n+1} - T_j^n}{\Delta t} = \alpha \frac{T_{j+1}^{n+1} - 2T_j^{n+1} + T_{j-1}^{n+1}}{(\Delta x)^2} \tag{5}$$

2-4 A Combined Implicit-Explicit Representation

The simple explicit, simple implicit and Crank-Nicolson methods are special cases of a general algorithm [3] given by

$$\frac{T_j^{n+1} - T_j^n}{\Delta t} = \alpha \frac{\theta \delta_X^2 T_j^{n+1} + (1-\theta)\delta_X^2 T_j^n}{(\Delta x)^2} \tag{6}$$

where θ is a weighting factor $(0 \le \theta \le 1)$. The simple explicit method corresponds to $\theta = 0$, the Crank-Nicolson methods corresponds $\theta = 1/2$ and the simple implicit method corresponds to $\theta = 1$.

2-5 Crank-Nicolson Method

When the fully explicit and implicit representations of the heat diffusion term are averaged, the scheme suggested by Crank-Nicolson [4] is

$$\frac{T_j^{n+1} - T_j^n}{\Delta t} = \alpha \frac{\delta_X^2 T_j^n + \delta_X^2 T_j^{n+1}}{2(\Delta x^2)} \tag{7}$$

2-6 Dufort-Frankel Method

It was suggested to avoid unstable algorithm of simple explicit scheme (Richardson method) by replacing T_j^n in the diffusion term with the time-average expression $(T_j^{n+1} + T_j^{n-1})/2$. The resulting is three-time-level scheme [5]

$$\frac{T_j^{n+1} - T_j^{n-1}}{2\Delta t} = \alpha \frac{T_{j+1}^n - T_j^{n-1} - T_j^{n-1} + T_{j-1}^n}{(\Delta x)^2} \tag{8}$$

2-7 Barakat-Clark Method

This method is known as alternating direction explicit (ADE) method [6]. The two-step scheme involves the simultaneous matching of two approximate solutions p_j^{n+1} and q_j^{n+1}. The two solutions are advanced separately, and at each time level, the solution to the difference equation is considered to be the average. For the heat diffusion equation, the algorithm is given by

$$\frac{p_j^{n+1}-p_j^n}{\Delta t}=\alpha\frac{p_{j-1}^{n+1}-p_j^{n+1}-p_j^n+p_{j+1}^n}{(\Delta x)^2} \tag{9a}$$

$$\frac{q_j^{n+1}-q_j^n}{\Delta t}=\alpha\frac{q_{j-1}^{n}-q_j^{n}-q_j^{n+1}+q_{j+1}^{n+1}}{(\Delta x)^2} \tag{9b}$$

$$T_j^{n+1}=\frac{1}{2}(p_j^{n+1}+q_j^{n+1}) \tag{9c}$$

2-8 Alternative Direction Implicit Method

ADI procedures discussed by [7, 8, and 9] avoids disadvantages of the previous methods and yet still mange to use a system of equations with a tridiagonal coefficient matrix for which the algorithm affords a straight forward solution. Essentially, the principle is to employ two difference equations which are used in turn over successive time-steps each of duration $\Delta t/2$. The usefulness of Taylor series expansions in developing and evaluating finite-difference representations for partial derivatives has been demonstrated. Several other techniques can also be used to develop difference expressions. Among these are polynomial fitting, the integral method, and control volume (alternatively called finite volume) analysis.

3-CONSISTENCY, STABILITY, AND CONVERGENCE

The first requirement that any scheme should meet is that of consistency. That is, it should be clear that $\lim_{\text{mesh}\to 0}(\text{PDE}-\text{FDE})=0$. This deals with the difference representation. It must also be possible to solve the difference equations in a manner that prevents the grows of errors. The numerical solution is invariably " rounded " to a finite number of digits in the arithmetic operations. This creates errors known as roundoff errors. Some solution algorithms contain a large number of dependent arithmetic operations. Even though a single roundoff error may be very small, certain algorithms permit the errors to grow to the point where they dominate the numerical solution. This must be avioded.

For marching problems, the errors will not grow if the solution scheme is stable. A stable scheme is thus defined as one for which errors from any source are not permitted to grow in the sequence of numerical procedures as the calculation proceeds from one marching step to the next. Thus, it is seen that an acceptable finite-difference representation for a marching problem must meet the conditions of consistency and stability. A scheme meeting these requirements for a marching problem is generally found to be convergent. Convergence here means that the solution to the finite-difference equation approaches the true solution to the PDE having the same initial and boundary conditions as the mesh is refined. Perhaps a more descriptive terminology for this type of convergence is " truncated convergence," since the word convergence is used in other contexts, as in "iteration convergence ." Lax was able to prove that given a properly posed initial value problem (governed by a linear PDE) and a finite-difference

approximation to it that satisfies the consistency condition, stability is the necessary and sufficient condition for convergence. This important result is as Lax's equivalence theorem. Although the theorem has been proved only for linear PDEs, computational work generally proceeds as though it where applicable also to nonlinear PDEs.

Although it is important to use a convergent algorithm in solving a PDE numerically, it is never possible to refine the mesh size to zero. Thus, calculations must be made on a finite grid, and there are errors in the numerical solution. These errors in the solution are referred to as discretization errors. More specifically, discretization error is the error in the solution to PDE caused by replacing the continuous problem by a discrete one and is defined as the difference between the exact solution of the PDE (roundoff-free) and the exact solution of the finite-difference equations(roundoff-free). Thus, the difference between the exact solution of the PDE and the computer solution is equal to the sum of the discretization error and the roundoff error associated with the finite-difference calculations. It can also be observed that the discretization error is the error in the solution caused by the truncation error in the difference representation of the PDE plus any error included by treatment of the boundary conditions

The influence of grid structure was determined by examining the limiting case (enclosure heating and cooling at vertical sides as well as perfectly insulated at horizontal sides) [10] with different grid spaces. Figure (1) shows the predicted stream functions for three different grid spaces at the mid-plane of the enclosure. The overall errors are 52.2 %, 18.6 %, and 6.0 % at the mid-plane of the cavity for the three different grid spaces. The results clearly indicate that the grid spacing must be sufficiently fine to allow the model to represent a physically meaningful situation. The temperature profiles at the mid-plane of the cavity for the same problem are shown in Figure (2). The results for 17 × 17 grid are not plotted for the sake of clearity. The overall errors are 4.4 %, 2.9 %, and 0.9 % for the three different grid spaces. The 9 × 9 spacing is more satisfactory for predicting the temperature than the stream function. The stream function indicates large errors when the node sizes are large, whereas the temperature shows relatively small errors even for a crude mesh as shown in Figures (1) and (2). This means that the temperature fields are relatively weak functions in the flow field and is one of the reasons why good results can be obtained for the average Nusselt numbers using relatively coarse grid.

Although the coordinate transformation decreases the overall numerical error, it increases the computational time by approximately 30 %. The boundary layer region is calculated more accurately by increasing the deformation parameter ε, but the central region of the cavity suffers some additional error. For the present problem there exists an optimal value of the parameter ε (approximately $0.7 < \varepsilon < 0.8$) [10]

The choice of the form of coordinate transformation may depend on the nature of the particular problems to be solved. Several useful transformations have been discussed (Roache, 1972; and Chenoweth and Paolucci, 1981) [11] & [12]. For natural convection in a cavity, the relation

$$r(\xi) = [1 + \tan[\frac{\pi\varepsilon}{2}(2\varepsilon - 1)] / \tan(\frac{\pi\varepsilon}{2})] / 2 \qquad (10)$$

has been recommended by Küblbeck et. al. [13]. Figure (3) shows a graph of this equation for several values of the deformation parameter ε .

4- FINITE-ELEMENT METHODS FOR PARTIAL DIFFERENTIAL EQUATIONS

The basic idea in the finite element method is to find the solution of a complicated problem by replacing it by a simple one. Since the actual problem is replaced by a simple one in finding the solution, this is due to find only an approximate solution rather than the exact solution. The existing mathematical tools will not be sufficient to find the exact solution (and sometimes, even an approximate solution) of most of the practical problems. Thus in the absence of any other convenient method to find even the approximate solution of a given problem, the finite element method is preferred. Moreover, in the finite element method, it will often be possible to improve or refine the approximate solution by spending more computational effort. In the finite element method, the solution region is considered as built up of many small, interconnected subregions called finite elements.

The underlying principle of the FEM is its ability to easily solve problems described by complex boundary shapes . the FEM was initially developed to calculate stress in irregular shaped objects and analyze structural problems in aircraft. Since its inception, the FEM has been found to be equally effective in nonstructural problems, particularly those in heat transfer and fluid dynamics.

Conventional FDMs are based on the assumption that truncated Tayler series expansions of the spatial derivatives yields adequate approximations to differential equations. Finite-difference algorithms display good accuracy in the limit as $\Delta x \rightarrow 0$. No such assumption is implied in the FEM; finite -element algorithms are based on finite Δx . This conceptual difference helps to explain the general superiority of the FEM over FDM on coarse grids; however, as $\Delta x \rightarrow 0$, the FEM also becomes more accurate (which is due to its convergent and consistent approximations).

Like, any analytical methods, the FEM is based on the series expansion of the functions themselves. In a typical series expansion, an infinite number of global basis functions (sines, cosines, etc.)span the entire domain. However, in the FEM, only a finite number of basis functions that are local in the nature (nonzero over only a small segment of the domain) are employed.

With the use of the local basis functions, the coefficient matrices that result from the approximation procedure of the governing equation became banded and sparse. FDM also procedure banded sparse matrices. However, the coefficients in the FEM vary from node to node, since nodal locations are arbitrary ;hence the resulting matrices become considerably fuller due to greater degree of coupling among nodes. For example, the Laplacian operator generates 3-,5-and 7-nodal point coupling for one- two-, and three-dimensional domains in a second -order FDM. In the FEM, the simplest basis function generates a 3-,9-, or 27-point coupling. In the addition, time derivative terms are coupled in the FEM, whereas they are not in most FDMs.

In the FEM a partial differential equation is reduced to a finite system of ordinary differential equations, which is then solved by a matrix solution techniques. Reduction of the governing equation is typically performed using either (1) the Rayleigh-Ritz method or (2) the method of weighted residuals (MWR). In the Rayleigh-Ritz method, variational calculus is used to formulate a variational statements of the problem. In

order to use the variational method, an appropriat integral over the problem domain must possess an extremum. In most instances, this extremum is based on energy concepts, that, is Lagragian multipliers. For simple problems, such as potential flow or conduction heat transfer, the variational formulation is easily established. However, for most practical problems , particularly when advection terms are present, variational principles cannot be developed. In the MWR, the governing equation is multiplied by a weighting function Wi, and the product is integrated over space(hence the term weighted residual) the MWR is a more general approach that permits a functional form of the dependent variables to be obtained for any transport equation regardless of its complexity. The method generates the same number of equations as unknowns. For N unknowns(numbers of node points), the domain is subdivided into N intervals of integration.

There several variations of the MWR. In the Galerkin procedure, the approximating function, Ni, for dependent variable is chosen to be the same as the weighting Wi. When the weighting function is not equal to the approximating function, other weighted residual methods are obtained- for example , least squares, collocation and spectral methods. The Galerkin approach is the most popular, and we will employ it in this comparison study. A discussion of other methods employed in the MWR can be found in Refs. [14], [15] & [16]. The development of spectral and pseudospectral methods(a combination of collocation and spectral) is discussed through Refs. [17], [18], [19]& [20]

A finite element analysis of any physical or engineering problem leads to a system of matrix equations. After incorporating the boundary conditions in the assembled system of equations, the final matrix equations are obtained. If the problem is nonlinear, the resulting matrix equations will also be nonlinear irrespective of the type of problem (equilibrium, eigenvalue or propagation problem). If the problem is nonlinear, some sort of an iterative procedure has to be used for finding the solution. For example, the matrix equations that result from the finite element analysis of a nonlinear equilibrium (or steady state) problem can be solved by using any of the following schemes [21,22]:

1. Newton-Raphson method
2. Continuation methods
3. Minimization methods
4. Perturbation methods

5-FINITE DIFFERENCE VERSUS FINITE ELEMENTS

5-1 Introduction

In the preceding sections of this paper, the applicability and effectiveness of both finite-difference and finite-element techniques in solving heat transfer and related transport problems have been demonstrated. The choice of which particular technique to use ultimately lies with the user. In general, one uses a simple technique to solve a simple problem and complex(or more sophisticated) technique to solve a difficult problem. There is no one best method for all problems. However, there are methods that have a wide degree of applicability for a general class of problems.

There are currently two major approaches used to numerically solve the partial differential equations associated with heat transfer problems-the finite difference method (FDM) and finite element method (FEM). An extensive amount of literature exists that delves into the intricate details of numerous algorithms associated with both methods. It is our intent in this section to illustrate the basic differences and similarities between the FDM and the FEM. More in-depth analysis can be found in the cited references.

The FDM has been used for many years in numerous applications. Examples of finite-difference applications can even be found in the works of Newton, Gauss, and Laplace. The study of such methods , particularly over the last 40 years, has resulted in a fast expansions of knowledge. The FEM, a relatively recent development in comparison, is becoming increasingly popular. Interestingly, the FEM is linked to finite-difference theory through its development of approximation schemes. Since it is impossible to cover all aspects of both finite -difference and finite element theory within a short paper, we shall limit our discussion to finite-difference and finite -element techniques commonly found in the literature.

A Tayler weak-statement (TWS) algorithm is used in conjunction with the FEM to examine errors common to FDM and FEM. A generalized mathematical statement is developed that shows the various terms associated with a particular technique that lead to error and /or damping of the true solution. The TWS algorithm provides a mathematical basis for establishing common error analyses in a wide variety of numerical methods.

5-2 One-Dimensional and Two-Dimensional Elements

To illustrate the differences in methodology and equation form between the FDM and the FEM, the finite -difference equivalent of the one-dimensional finite-element algorithm derived for both linear and quadratic basis functions. The quadrilateral element is a four-sided figure that contains four nodes located at the vertices in a linear configuration, eight or nine nodes in a quadratic element, and 12 nodes in a cubic element. In the its simplest form, the quadrilateral becomes a rectangular element with boundaries of the element parallel to a coordinate system. Further extension of the element, using the local natural coordinate system, results in a generalized quadrilateral of which the rectangle is a subset.

Analysis of the finite-element approximation on a two-dimensional rectangular grid is summarized in Table 2 , following procedures discussed in Pinder and Gray [1]. Grouping elements of coefficient matrices allows the equivalent finite- difference approximation to be generated. The coefficient multiplying each derivative is written as an integration formula; the finite-element technique can be interpreted as a finite difference discretization in one spatial direction integrated over the other direction. The truncation error associated with the FEM is of higher order for advection term but equivalent to the FDM for the diffusion term.

For irregular grids, the error associated with linear basis functions is of the same order as the finite-difference truncation error on the same mesh. The use of quadratic basis functions leads to improve accuracy. In most finite-difference procedures the accuracy of the solution is the same at all nodes within the solution domain. In a two-dimensional finite-element solution using eight noded quadratic elements, accuracy is

TABLE 2. Rectangular Grid — FEM and FDM Comparisons[a]

Term	$\frac{\partial c}{\partial t}$	$u\frac{\partial c}{\partial x}$	$w\frac{\partial c}{\partial z}$
Finite-Element Representation	$\frac{\Delta x\,\Delta z}{36}\left\{\left[\frac{dc_{-1,1}}{dt}+4\frac{dc_{0,1}}{dt}+\frac{dc_{1,1}}{dt}\right]+4\left[\frac{dc_{-1,0}}{dt}+4\frac{dc_{0,0}}{dt}+\frac{dc_{1,0}}{dt}\right]+\left[\frac{dc_{-1,-1}}{dt}+4\frac{dc_{0,-1}}{dt}+\frac{dc_{1,-1}}{dt}\right]\right\}$	$u\frac{\Delta x\,\Delta z}{6}\left\{\left[\frac{c_{1,1}-c_{-1,1}}{2\Delta x}\right]+4\left[\frac{c_{1,0}-c_{-1,0}}{2\Delta x}\right]+\left[\frac{c_{1,-1}-c_{-1,-1}}{2\Delta x}\right]\right\}$	$w\frac{\Delta x\,\Delta z}{6}\left\{\left[\frac{c_{1,1}-c_{1,-1}}{2\Delta z}\right]+4\left[\frac{c_{0,1}-c_{0,-1}}{2\Delta z}\right]+\left[\frac{c_{-1,1}-c_{-1,-1}}{2\Delta z}\right]\right\}$
Numerical differentiation formula used	—	$\frac{\partial c_{0,k}}{\partial x}=\frac{c_{1,k}-c_{-1,k}}{2\Delta x}-\frac{1}{6}(\Delta x)^2\frac{\partial^3 c_{0,k}}{\partial x^3}$ $k=-1,0,1$ 2nd-order accurate	$\frac{\partial c_{j,0}}{\partial z}=\frac{c_{j,1}-c_{j,-1}}{2\Delta x}-\frac{1}{6}(\Delta x)^2\frac{3c_{j,0}}{(\Delta z)^3}$ $j=-1,0,1$ 2nd-order accurate
Numerical integration formula used	$\int\frac{\partial c}{\partial t}dx\,dz=\frac{\Delta x\,\Delta z}{9}\left\{\left[\frac{ac_{-1,1}}{\partial t}+4\frac{\partial c_{0,1}}{\partial t}+\frac{\partial c_{1,1}}{\partial t}\right]+4\left[\frac{\partial c_{-1,0}}{\partial t}+4\frac{\partial c_{0,0}}{\partial t}+\frac{\partial c_{1,0}}{\partial t}\right]+\left[\frac{\partial c_{-1,-1}}{\partial t}+4\frac{\partial c_{0,-1}}{\partial t}+\frac{\partial c_{1,-1}}{\partial t}\right]\right\}-\frac{\Delta x(\Delta z)^5}{45}\frac{\partial^4}{\partial z^4}\left(\frac{\partial c}{\partial t}\right)-\frac{\Delta z(\Delta x)^5}{45}\frac{\partial^4}{\partial x^4}\left(\frac{\partial c}{\partial t}\right)$ 4th-order accurate (2-dimensional Simpson's rule)	$\int\frac{\partial c_{0,k}}{\partial x}dz=\frac{\Delta z}{3}\left\{\frac{\partial c_{0,-1}}{\partial x}+4\frac{\partial c_{0,0}}{\partial x}+\frac{\partial c_{0,1}}{\partial x}\right\}-\frac{(\Delta z)^5}{90}\frac{\partial^5 c}{\partial x\,\partial z^4}$ 4th-order accurate (1-dimensional Simpson's rule)	$\int\frac{\partial^2 c}{\partial x^2}dx=\frac{\Delta x}{3}\left\{\frac{\partial^2 c_{-1,0}}{\partial x^2}+4\frac{\partial^2 c_{0,0}}{\partial z^2}+\frac{\partial^2 c_{1,0}}{\partial z^2}\right\}-\frac{(\Delta x)^5}{90}\frac{\partial^6 c}{\partial^4\,\partial z^2}$ 4th-order accurate (1-dimensional Simpson's rule)

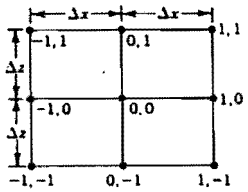

$-D\frac{\partial^2 c}{\partial x^2}$	$-D\frac{\partial^2 c}{\partial z^2}$	kc
$-D\frac{\Delta x\,\Delta z}{6}\left\{\left[\frac{c_{1,1}-2c_{0,1}+c_{-1,1}}{(\Delta x)^2}\right]+4\left[\frac{c_{1,0}-2c_{0,0}+c_{-1,0}}{(\Delta x)^2}\right]+\left[\frac{c_{1,-1}-2c_{0,-1}+c_{-1,-1}}{(\Delta x)^2}\right]\right\}$	$-D\frac{\Delta x\,\Delta z}{6}\left\{\left[\frac{c_{1,1}-2c_{1,0}+c_{1,-1}}{(\Delta z)^2}\right]+4\left[\frac{c_{0,1}-2c_{0,0}+c_{0,-1}}{(\Delta z)^2}\right]+\left[\frac{c_{-1,1}-2c_{-1,0}+c_{-1,-1}}{(\Delta z)^2}\right]\right\}$	$k\frac{\Delta x\,\Delta z}{36}\{[c_{-1,1}+4c_{0,1}+c_{1,1}]+4[c_{-1,0}+4c_{0,0}+c_{1,0}]+[c_{-1,-1}+4c_{0,-1}+c_{1,-1}]\}$
$\frac{\partial^2 c_{0,k}}{\partial x^2}=\frac{c_{1,k}-2c_{0,k}+c_{-1,k}}{(\Delta x)^2}-\frac{1}{12}(\Delta x)^2\frac{\partial^4 c}{\partial x^4}$ $k=-1,0,1$ 2nd-order accurate	$\frac{\partial^2 c_{j,0}}{\partial z^2}=\frac{c_{j,1}-2c_{j,0}+c_{j,-1}}{(\Delta z)^2}-\frac{1}{12}(\Delta z)^2\frac{\partial^4 c}{\partial z^4}$ $j=-1,0,1$ 2nd-order accurate	
$\int\frac{\partial^2 c_{0,k}}{\partial x^2}dz=\frac{\Delta z}{3}\left\{\frac{\partial^2 c_{0,-1}}{\partial x^2}+4\frac{\partial^2 c_{0,0}}{\partial x^2}+\frac{\partial^2 c_{0,1}}{\partial x^2}\right\}-\frac{\Delta z^5}{90}\frac{\partial^6 c}{\partial x^2\,\partial z^4}$ 4th-order accurate (1-dimensional Simpson's rule)	$\int\frac{\partial c_{j,0}}{\partial z}dx=\frac{\Delta x}{3}\left\{\frac{\partial c_{-1,0}}{\partial z}+4\frac{\partial c_{0,0}}{\partial z}+\frac{\partial c_{1,0}}{\partial x}\right\}-\frac{\Delta x^5}{90}\frac{\partial^5 c}{\partial z\,\partial x^4}$ 4th-order accurate (1-dimensional Simpson's rule)	$\int c\,dx\,dz=\frac{\Delta x\,\Delta z}{9}\{[c_{-1,1}+4c_{0,1}+c_{1,1}]+4[c_{-1,0}+4c_{0,0}+c_{1,0}]+[c_{-1,-1}+4c_{0,-1}+c_{1,-1}]\}-\frac{\Delta x(\Delta z)^5}{45}\frac{\partial^4 c}{\partial z^4}-\frac{\Delta z(\Delta x)^5}{45}\frac{\partial^4 c}{\partial x^4}$

[a]Source: Pinder and Grey[1]

improved at the corner nodes. The use of nine-nodded elements improves solution accuracy slightly more.

5-3 The Control-Volume Method

A numerical approach that tends to fit between the conventional FDM and FEM is the control-volume method. In some instances, this method is more accurate than the FDM, but it does not have the flexibility of the FEM. In this particular scheme, the differential equation is integrated over the interval $[\, x_{i-\frac{1}{2}}, x_{i+\frac{1}{2}} \,]$, where x_i is the node-location (grid center). as in the FEM, the integration reduces the differential equation by one order.

5-4 Stability Analysis-Computational Dispersion and Diffusion

There are two principle types of errors that occur as a result if the discretization processes:(1) computational dispersion and (2) computational diffusion. Computational dispersion arises from the numerical approximation of a steep gradient, usually associated with a large advection term. Computational diffusion, also known as artificial diffusion or damping, occurs as a result of the spatial truncation error of a method. Dispersion errors appear as waves, or oscillations, of negative and positive values that propagate as numerical solution is calculated . For example, most numerical methods cannot accurately calculate the advection of a square step (or shock front). An example of computational diffusion is the amount of damping inherent in upwind differencing techniques. In this instance, upwind methods eliminate dispersion errors but develop excessive diffusion errors (even though the solution is "stable" and smooth). Recall that in the one-dimensional, numerical instability occurs in the central-difference method but is improved in the upwind scheme. Using asymmetric weighting functions, a form of upwinding can also be applied to the FEM.

The following equation is commonly called the advection equation.

$$\frac{\partial \phi}{\partial t} + u\frac{\partial \phi}{\partial x} = 0 \qquad (11)$$

where ϕ is the transport variable, u is the velocity.

A one -dimensional cosine hill distribution is advected over a specified distance as shown in Fig. (4). A constant velocity is imposed on the distribution. The solution domain consists of 33 nodes; the initial distribution is spanned over nodes (Fig.(4)). The solution is stopped before it reaches the right-hand boundary, i.e., before it is advected out of the domain ($\frac{\partial \phi}{\partial x} = 0.$) The exact solution is shown by the dashed line; the Crank-Nicolson centered FDM and both the linear and quadratic FEMs are displayed. The Courant number C, varies from 0.4 to 1.6. The FEM yields excellent agreement for C=0.4 ; the FDM shows a sizable trailing wake(dispersion error =12%), slight damping of the peak value, and lagging of solution, At $C \geq 0.8$, the effect of the increased velocity is evident in both the FDM and FEM; however, the FDM result are markedly worse.
An understanding of the reason for the difference in results requires a closer examination of both methods.

The equivalent difference relation for the advection equation using linear finite element is

$$\frac{1}{6}(\phi i-1+4\phi i+\phi i+1)+U\left(\frac{\phi i+1-\phi i-1}{2\Delta x}\right)=0 \qquad (12)$$

which is the familiar chapeau function for constant mesh interval Δx and constant velocity u=U. Performing a Tayler series expansion about $x = x_i$ on Eq.12 produces the relation

$$\frac{\partial\phi}{\partial t}+U\frac{\partial\phi}{\partial x}-\frac{U(\Delta x)^4}{180}\frac{\partial^5\phi}{\partial x^5}+....=0 \qquad (13)$$

The truncation error shows the finite-element approximation to be fourth-order-accurate in space. In comparison, the FDM is written as

$$\phi i+U\left(\frac{\phi i+1-\phi i-1}{2\Delta x}\right)=0 \qquad (14)$$

and yields a truncation error of second order accuracy in space,

$$\frac{\partial\phi}{\partial t}+U\frac{\partial\phi}{\partial x}-\frac{U(\Delta x)^2}{12}\frac{\partial^3\phi}{\partial x^3}+....=0 \qquad (15)$$

The higher loss in peak value of the traveling distribution in the (Crank-Nicolson) FDM is partially attributable to its lower order spatial accuracy.
Table 3 lists Courant stability limits and phase-velocity ratios for both the FDM and FEM using various time differentiation schemes[23]

5.5 Comparison Between FEM and FDM

The answer to which method should be employed ultimately lies with the user. Which method is best depends upon the problem to be solved; weather there are singularities or discontinuities; regular or irregular boundaries; the necessity for mesh refinement; and so on. A very expedient method for one-dimensional problems may not be appropriate for two or three-dimensional problems. For example , three-dimensional FEMs become very costly and storage intensive compared to FDMs; however, for one or two-dimensional problems, FEMs are competitive with and usually superior to conventional FDMs . Low-order methods, such as linear finite elements or simple finite differences, are best for singularity problems; high order methods, e.g., quadratic finite elements, are better suited to problems with smooth solutions. Once the mesh , or nodal discretization of the problem domain, is established, the manner in which the equivalent algebraic equations are solved (iteratively versus direct) also influences the choice of a method.

In summary, FDMs are simple to formulate, can easily be extended to two or three-dimensions, and require considerably less computational work than finite elements (for equivalent nodes). The recent introduction of boundary-fitted coordinates, coupled with finite-differencing, yields fairly reasonable solutions for domains with irregular boundaries.

In Galerkin method, irregular geometries are easily handled; small mesh sizes can be used in those regions where the solution changes significantly. Derivative or flux-type boundary conditions are automatically incorporated in Garlerkin methods without

TABLE 3 : Group Velocity Comparisons for Solving $\partial\phi/\partial t + u(\partial\phi/\partial x) = 0$

Numerical Scheme	Equation Form	Stability[a]	(Numerical/Theoretical) Group Velocity Ratio[b, c] R
FDM	$\frac{\phi_i^{n+1} - \phi_i^n}{\Delta t} + u\left(\frac{\phi_i^n - \phi_{i-1}^n}{\Delta x}\right) = 0$	$C \le 1$	$\frac{(1 - C)\cos r + C}{[1 + C(\cos r - 1)]^2 + (C \sin r)^2}$
Lax-Wendroff FDM	$\frac{\phi_i^{n+1} - \phi_i^n}{\Delta t} + u\left(\frac{\phi_{i+1}^n - \phi_{i-1}^n}{2\Delta x}\right) - \frac{u^2 \Delta t}{2}\left(\frac{\phi_{i+1}^n - 2\phi_i^n + \phi_{i-1}^n}{(\Delta x)^2}\right) = 0$	$C \le 1$	$\frac{\left[1 - 2(C \sin r/2)^2\right]\cos r + (C \sin r)^2}{\left[1 - 2(C \sin r/2)^2\right]^2 + (C \sin r)^2}$
FDM	$\frac{\phi_i^{n+1} - \phi_i^{n-1}}{2\Delta t} + u\left(\frac{\phi_{i+1}^n - \phi_{i-1}^n}{2\Delta x}\right) = 0$	$C \le 1$	$\frac{\pm\cos r}{\left[1 - (C \sin r)^2\right]^{1/2}}$
FDM	$\frac{\phi_i^{n+1} - \phi_i^{n-1}}{2\Delta t} + \frac{u}{3}\left[4\left(\frac{\phi_{i+1}^n - \phi_{i-1}^n}{2\Delta x}\right) - \left(\frac{\phi_{i+2}^n - \phi_{i-2}^n}{4\Delta x}\right)\right] = 0$	$C \le 0.729$	$\frac{\pm\frac{1}{3}(4\cos r - \cos 2r)}{\left[1 - C^2\left(\frac{4}{3}\sin r - \frac{1}{6}\sin 2r\right)^2\right]^{1/2}}$
Linear FEM	$\frac{1}{6}\left[\left(\frac{\phi_{i-1}^{n+1} - \phi_{i-1}^{n-1}}{2\Delta t}\right) + 4\left(\frac{\phi_i^{n+1} - \phi_i^{n-1}}{2\Delta t}\right) + \left(\frac{\phi_{i+1}^{n+1} - \phi_{i+1}^{n-1}}{2\Delta t}\right)\right] + u\left(\frac{\phi_{i+1}^n - \phi_{i-1}^n}{2\Delta x}\right) = 0$	$C \le \frac{1}{\sqrt{3}}$	$\frac{\pm 3(1 + 2\cos r)}{(\cos r + 2)\left[(\cos r + 2)^2 - (3C \sin r)^2\right]^{1/2}}$
Crank-Nicolson FDM	$\frac{\phi_i^{n+1} - \phi_i^n}{\Delta t} + \frac{u}{2}\left(\frac{\phi_{i+1}^{n+1} - \phi_{i-1}^{n+1}}{2\Delta x}\right) + \frac{u}{2}\left(\frac{\phi_{i+1}^n - \phi_{i-1}^n}{2\Delta x}\right) = 0$	∞	$\frac{\cos r}{1 + (C/2 \sin r)^2}$
Crank-Nicolson FEM	$\frac{1}{6}\left[\left(\frac{\phi_{i-1}^{n+1} - \phi_{i-1}^n}{\Delta t}\right) + 4\left(\frac{\phi_i^{n+1} - \phi_i^n}{\Delta t}\right) + \left(\frac{\phi_{i+1}^{n+1} - \phi_{i+1}^n}{\Delta t}\right) + \frac{u}{2}\left(\frac{\phi_{i+1}^{n+1} - \phi_{i-1}^{n+1}}{2\Delta x}\right) + \frac{u}{2}\left(\frac{\phi_{i+1}^n - \phi_{i-1}^n}{2\Delta x}\right) = 0$	∞	$\frac{3(1 + 2\cos r)}{(\cos r + 2)^2 + \left(\frac{1}{2}C \sin r\right)^2}$

[a] $C = u\Delta t/\Delta x$

[b] Group velocity $= \partial\Lambda/\partial\omega$, Λ = real component of angular frequency; $R = (\partial\Lambda_{num}/\partial\omega)/(\partial\Lambda_{theor}/\partial\omega)$

[c] $r = \omega\Delta x$

Source: Cathers and O'Connor. [23]

diminishing the accuracy of the overall solution. In the FDM, boundary conditions are generally resolved following solution of the domain interior, often using simple one sided approximations of lower-order accuracy . In some flow situations, lower-order boundary approximations must be used with the FDM to achieve stable solutions. Higher order approximations for the overall solution are more easily generated in the FEM and do not require special treatment near the boundaries. Finally, the FEM generates numerical approximations that satisfy certain global conservation laws, independent of the boundary conditions and geometry, which lead to computationally well-behaved results.

The biggest drawback to the FEM is that it is inherently an implicit method (since the time derivatives are coupled in the mass matrix). Inversion of the mass matrix, if an explicit scheme is used, is not practical except for small problems. Hence, the trapezoidal rule is usually employed to advance over one time step; banded Gaussian elimination or iterative techniques are generally used to solve the linear system of algebraic equations. Although the mass matrix terms can be lumped to permit explicit integration, loss of accuracy can become significant.

Large FEM codes cannot be totally contained in the CPU memory of even the largest computers. Hence, peripheral storage on tapes and disks, which also leads to large I/O times, is necessary . In addition, solution of nonlinear problems normally requires that many of the Garlerkin integrals (matrices) be recalculated at each time step; in linear problems, they can be calculated once and stored for later use. Table 4 shows the amount of computational work and storage associated with the implicit central FDM using alternating direction procedures and the FEM using linear and quadratic elements for a 30 x 30 element two-dimensional mesh Ref.[24]. In the final analysis, the numerical modeler should be knowledgeable about several methods. However, modelers who attempt to learn all the available methods and techniques currently discussed in the literature may never get back to solving their problems. The FDM is easy to learn and implement and provides good results for simple geometries. It is a powerful technique that can be applied to a wide variety of problems with simple or complex geometries.

TABLE 4. Work Comparisons for an Ne × Ne Grid[a]

	Local Nodes	Estimate	Estimate	n	Operation Count $\times 10^{-6}$	Matrix Storage
		Work for Equivalent Number of Nodes, $n = Ne_j = 2Ne_2$				
FDM, ADI	3	$6i\,Ne_1^2$	$6in^2$	30	0.11	$3\,Ne_1 = 90$
FEM, linear	4	Ne_1^4	n^4	30	0.81	$2\,Ne_1^4 = 1.6 \times 10^6$
FEM, quadratic	8	$27\,Ne_2^4$	$1.7n^4$	15	1.4	$18\,Ne_2^3 = 0.061 \times 10^6$
FEM, quadratic	9	$64\,Ne_2^4$	$4n^4$	15	3.2	$32\,Ne_2^3 = 0.11 \times 10^6$
		Work for Equivalent Accuracy, $n = Ne_1$, $Ne_1^2 = Ne_2^3$				
FDM, ADI	3	$6i\,Ne_1^2$	$6in^2$	10	0.012	$3\,Ne_1 = 30$
FEM, linear	4	Ne_1^4	n^4	10	0.010	$2\,Ne_1^4 = 20000$
FEM, quadratic	8	$27\,Ne_2^4$	$27n^{8/3}$	4.64	0.013	$18\,Ne_2^3 = 1800$
FEM, quadratic	9	$64Ne_2^4$	$64n^{8/3}$	4.64	0.030	$32\,Ne_2^3 = 3200$

[a] i = no. of iterations = 20; Ne_j = number of elements in one direction; $j = 1$ (linear), $j = 2$ (quadratic). Work is the number of multiplications for a LU decomposition; for the ADI method, the work estimate is for a fore-and-aft sweep.

Source: Finlayson[24]

6. FINITE ANALYTICAL METHOD

The basic idea of the finite analytic method is the incorporation of a local analytic solution in the numerical solution of ordinary or partial differential equations. The finite analytic method decomposes the total region of a problem governed by differential equations into a number of small elements in which local analytic solutions are obtained due to locally simple geometry, equations, and boundary conditions. When the local analytic solution is evaluated at an interior node, it gives an algebraic equation relating the evaluated interior nodal value to its neighboring nodal values. The discrete model of the total problem is obtained by assembling and overlapping all local analytic solutions. The finite analytic numerical solution is then achieved by solving the system of algebraic equations assembled from these analytic solutions derived for each element. In the case of nonlinear problems the governing differential equation can be locally linearized and solved analytically. In this fashion the overall nonlinear effect can still be approximately preserved by the assembly of locally analytic-solutions.

The finite analytic (FA) method thus differs from the finite-difference (FD) and finite-element (FE) methods in that the approximate algebraic analogy of the governing differential equation is obtained from an analytic solution. To illustrate the basic principles one can consider a two-dimensional elliptic partial differential equation (PDE), e.g., $L(\phi) = g$, where L is a linear or nonlinear partial differential operator and g is an inhomogeneous term that depends only on the independent variables, taken to be x and y. The PDE is to be solved in the region D shown in Fig. 5. Let the boundary conditions be specified so that the problem is well-posed. The region D is subdivided into small rectangles. The intersections from the nodal points $1,2,3,...,i-1,i,i+1,...,I$ and $1,2,3,...,j-1,j,j+1,...,J$. A typical subregion of the problem with node point $P(i,j)$ may be surrounded by the neighboring node points EC (east center), WC (west center), SC (south center), NC (north center), NE (northeast), NW (northwest), SE (southeast), and SW (southwest), which correspond to points $(i+1,j),(i-1,j),(i,j-1),(i,j+1)$, $(i+1,j+1)$, $(i+1,j+1)$, $(i-1,j+1),(i+1,j-1)$, and $(i-1,j-1)$, respectively.

One D has been subdivided into simple rectangular subregions, an analytic solution in each subregion may be obtained. Let the linear or linearized governing equation in a simple subregion of $2h \times 2k$ be $L(\phi) = g$, so that an analytic solution can be obtained for the subregion as a function of the boundary conditions, or

$$\phi = f[\phi_N(x), \phi_S(x), \phi_E(y), \phi_W(y), h, k, x, y, g] \tag{16}$$

where ϕ_N, ϕ_S, ϕ_E, and ϕ_W are, respectively, the northern, southern, eastern, and western boundary conditions of the subregion, and 2h and 2k are, respectively, the x and y lengths of the subregion. For numerical purposes, the boundary functions ϕ_S, ϕ_E, and ϕ_W may be approximately expressed in terms of the nodal values along the boundary, e.g., $\phi_S = \phi_S(\phi_{SE}, \phi_{SC}, \phi_{SW}, x)$ as shown. Substituting such boundary conditions into Eq. (16), including all four boundary surfaces, one has

$$\phi = f(\phi_{EC}, \phi_{WC}, \phi_{NC}, \phi_{SC}, \phi_{NE}, \phi_{NW}, \phi_{SW}, \phi_{SE}, x, y, h, k, g) \qquad (17)$$

Equation (17) represents the analytic solution and contains a dependence on the local boundary values, $\phi_{EC}, \phi_{WC}, \ldots$, etc. Extracting this dependence explicitly, one can obtain the nine-point FA formula for ϕ_p when Eq. (17) is evaluated at point P. This can be written in the form

$$\phi_p = C_{EC}\phi_{EC} + C_{WC}\phi_{WC} + C_{NC}\phi_{NC} + \ldots + C_{SW}\phi_{SW} + C_{SE}\phi_{SE} + C_{Pg}P \qquad (18)$$

Here the C's are known analytic coefficients multiplying the corresponding neighboring nodal values ϕ_{EC}, ϕ_{WC}, etc. [25]

In general, Eq. (18) may be derived for each unknown nodal point (i, j) in internal subregions to form a set of algebraic equations relating the interior node to its neighboring nodes. The system of algebraic equations can be solved in conjunction with the boundary conditions of the problem to provide the FA numerical solution of the problem, the complex boundary conditions can be converted into an algebraic form with a finite-difference approximation relating the boundary node to the interior nodes. This is the essence of the FA method.

Convective, conductive, and radiative heat transfer problems, in general, are described by a set of partial differential equations that are a mathematical formulation of the laws of conservation of mass, momentum, and energy.

6.1 Comparison of Finite Analytic And Finite-Difference Coefficients For Heat Equation

Figure 6 shows the comparison of the FA coefficients with various FD coefficients as a function of λ for $\lambda = 0.01$-10. It should first be remarked that the FA formula is obtained without approximating the derivatives of partial differential equations. In Fig. (6) the coefficient C_{SC}, C_{SE}, and C_{SW} are shown as dashed lines for the FD explicit method and as a solid line for the FA method. C_{EC} and C_{WC} are zero from the definition of the FD explicit formula. Comparison of the values of the coefficients in the FD explicit and FA solutions shows that the corresponding coefficients behave qualitatively the same for $\lambda = \Delta t/\Delta x^2 < 0.5$, while they disagree for $\lambda > 0.5$, since as λ increases the coefficient C_{SC} of the FD ($\theta = 0$) solution becomes negative and the FD coefficients C_{SE} and C_{SW} become infinite. The existence of negative and infinite values explains why the numerical instability occurs for the FD explicit method when $\lambda > 0.5$. On the other hand, as the λ value approaches zero, the coefficient of the FD ($\theta = 0$) explicit method approaches the FA value, thus providing an agreeable, accurate numerical solution.

Now consider the FD ($\theta = 1$) implicit method. The coefficients in this case can be

obtained with a backward difference in the time derivative ϕ_t and a central difference in the spatial derivative ϕ_{xx}. Figure (6) provides the variation of the FD coefficients C_{SC}, C_{EC}, and C_{WC} as a function of λ. Although these FD coefficients agree qualitatively with the corresponding FA coefficients, there are large differences even at moderate values of λ. This means that the FD implicit scheme is stable but is not accurate. Indeed, ignoring the influence of initial nodal values ϕ_{SE} and ϕ_{SW} (i.e., $C_{SW} = C_{SE} = 0$) on the nodal value ϕ_P is understandably undesirable. On the contrary, each of the finite analytic coefficients is never identically zero for all ranges of λ.

Other improved finite difference formulas such as the Crank-Nicolson (θ = 1/2) and Forsythe-Wasow ($\theta = (6\lambda\text{-}1)/12\lambda$] formulas behave much better than the explicit or implicit FD methods, because they include the influence of the nodal values ϕ_{SE} and ϕ_{SW} in the FD formula. That is, the FD coefficients C_{SW} and C_{SE} are never identically zero as in the implicit FD form and never become infinite at the large value of λ as in the explicit FD form. The comparison of C_{SW} and C_{SE} is shown in Fig. (6). The FD coefficients C_{SW} and C_{SE} qualitatively agree with the FA value up to $\lambda = 2$; beyond that there is a discrepancy between the FD and FA values. The other FD coefficients, C_{SC}, C_{EC}, and C_{WC}, for $\theta = (6\lambda\text{-}1)/12\lambda$ are shown in Fig. (6). Figure (6) shows that the C_{EC} and C_{WC} coefficients for both cases agree well with corresponding FA coefficients except where $\lambda < 0.2$, where the coefficients for Forsythe-Wasow method fall below zero, which is contrary to all other cases. On the other hand, the FD coefficient C_{SC} agrees well with the FA C_{SC} only for $\lambda < 1$; beyond that the coefficient for both the Crank-Nicolson and Forsythe-Wasow methods becomes negative, which disagrees with the FA coefficient. Further comparison shows that for the Crank-Nicolson formula, if λ is approximately 0.7, the FD solution agrees best with the present FA solutions, and that for the Forsythe-Wasow formula, if λ is set to $1/\sqrt{20}$, it provides the best agreement with the present FA solution. Indeed it has been shown [26] that for the Forsythe-Wasow formula if λ is set to $1/\sqrt{20}$ the error is reduced to $o(\Delta x^6)$. From the above comparison the finite analytic solution is shown to be the best for all ranges of λ values, while the Crank-Nicolson and Forsythe-Wasow formula do improve the accuracy of the FD formula but only for some particular value of λ. The FA solution can be used to examine or to explain the instability behavior and the accuracy of various finite-difference approximations.

6.2 Applications of Finite Analytic Solutions

6.2.1 Ordinary Differential Problems

One can apply to linear and nonlinear ordinary differential equations. This was studied by Li and Chen [27] and by Chen, Sheikholeslami and Bhiladvala [28]

6.2.2 Natural Convection Problems

The finite analytic solution was applied by Chen and Talaie [29,30] to study steady and unsteady natural convection in rectangular enclosures.

6.2.3 Flow and Heat Transfer Problem

The finite analytic method was used by Chen and Yoon [31] and Chen and Chang [32] to solve turbulent separated flow and heat transfer in rectangular and cylindrical cavities and flow behind steps. Further applications of the finite analytic method in flow problems are given in references [33-37].

6.2.4 Supersonic Flow and Shock Wave Problems

The finite analytic solution for the hyperbolic equation in supersonic flow was obtained by Chen and Chen [38] using the analytic solution obtained from the theory of characteristics. The shock wave in an arbitrary convergent and divergent channel was predicted by the finite analytic method.

6.3 Summary

One can introduce the finite analytic method and apply to the solution of heat transfer problems. The finite analytic method differs from other methods in that it utilizes the analytic solution of the governing equation for an element in constructing an algebraic representation of the partial or ordinary differential equation. Consequently, because of the analytic nature of the solution for the well-posed problem, the numerical solution is stable and relatively accurate.

The finite analytic coefficients in the finite analytic algebraic equation are obtained from the analytic solution. They at first appear to be complicated and time-consuming to evaluate. However, in practice, the time consumed in tabulating these finite analytic coefficients is a small portion of the total computation time. The stability and accuracy of the finite analytic method provides an attractive alternative means of obtaining numerical solutions in heat transfer problems.

7. METHODS OF MONTE CARLO

Monte Carlo, a branch of experimental mathematics, is a method of directly simulating mathematical relations by random processes. In physics, the Monte Carlo method has been used to solve numerous types of diffusion problems and has enjoyed a great deal of attention [39].

In heat transfer, interest has been relatively small. Radiation and conduction have dominated the use of the Monte Carlo method, while its application to convective problems has been insignificant, despite the fact that, for instance, the transport of energy in a turbulent flow depends on random processes. Future research in this area appears to be promising.

The Monte Carlo method, as stated earlier, is a statistical approach to the solution of multiple integrals of the type

$$I(\xi_1,\xi_2,\ldots,\xi_k) = \int_0^1\int_0^1\cdots\int_0^1 w(\xi_1,\xi_2,\ldots,\xi_k)\,dP_1(\xi_1)\,dP_2(\xi_2)\ldots dP_k(\xi_k) \qquad (19a)$$

where $\xi_1, \xi_2, \ldots, \xi_k$ are related to random variables and $P_1(\xi_1)$, $P_2(\xi_1)$, $\ldots$, $P_k(\xi_k)$, are the corresponding cumulative distribution or probability distribution functions. If η_k is a random variable, then

$$P_k(\xi_k) = \text{probability}\,(\eta_k < \xi_k) \qquad (19b)$$

The main criticism of the Mote Carlo method concerns its inefficiency in dealing competitively with mathematical problems whenever there is an alternative solution. Understandably, this is true for a great many problems. However, the Monte Carlo method is extremely useful when (1) there is no other convenient method, (2) a simple procedure is needed to check the validity of a new method, and (3) in some instances, a computationally faster procedure is needed. Indeed, it is refreshing to see that the Monte Carlo procedure, for some problems, can result in a much faster solution than, for example, the finite-difference method.

7.1 Definite Integrals

The Monte Carlo method provides a vehicle to numerically evaluate multiple integrals. Extensive details are available in Refs. [40] and [41]. Monte Carlo becomes indispensable whenever multiple integrals have many variables and cannot be evaluated efficiently by standard numerical techniques. This condition exists in many radiation problems.

7.2 Transient Conduction

The solution for transient heat conduction problems requires the assignment of a time increment to each step of a random walk. However, the Monte Carlo procedure for a floating random walk is different from that for the random walk with a fixed step size. The incremental time assigned to a random walk with a fixed step size is constant everywhere in a homogenous domain. The floating random walk procedure described earlier uses a combination of large radial steps, $r_i > r_{min}$, and small incremental steps, $r_i < r_{min}$, with the duration of a step depending on the size of the step. Zinsmeister and Pan [42] suggested a hybrid Monte Carlo method to calculate temperature in the entire field. First, calculation of temperature is carried out, using Monte Carlo on the boundary of an inscribed regular domain, and then the internal temperature is computed analytically.

An important feature of Monte Carlo is its simplicity. It uses very little computer memory and requires minimal computer programming effort. Despite common belief, a Monte Carlo method can produce solutions to a class of thermal conduction problems faster than any conventional numerical method. Let us consider a situation for which the temperature should be determined repeatedly at a few internal points in a region for different boundary temperatures. Only a small portion of computer memory is needed to keep, and to store for subsequent use, a record of the number of random walks terminated at any given boundary point.

7.3 Convection

Generally, the Monte Carlo solution of convection problems is similar to that described earlier for conduction applications. All discussions concerning the Monte Carlo method with a fixed step size, and in some instances with a variable step size, apply equally to convection problems. The class of convection problems suitable for Monte Carlo are linear, are decoupled from the momentum equations, and have a known velocity field. Information concerning nonlinear and/or coupled problems are rare.

7.4 Radiation

Radiation problems posses a form ideally suited for Monte Carlo application, since it provides a vehicle to numerically evaluate multiple integrals. The integral that governs the emission of radiant energy depends on various parameters such as wavelength, angle of emission, and the nature of the medium [43-46]. Also, different integrals govern the reflection and scattering processes. Preliminary attention is directed to the study of radiant exchange between surfaces in the absence of a participating, medium.

7.5 Application to Absorbing and Emitting Media

The procedure described for radiation exchange between different surfaces in the presence of a nonparticipating medium applies equally to participating media with some modification. Indeed, Monte Carlo can accommodate generalized radiation problems with a few approximations. Unlike analytical schemes, Monte Carlo does not require numerous assumptions concerning the surface properties (e.g., black or gray, specular or diffuse) and gas properties (opaque or transparent, gray, isothermal, thick or thin, etc.) to achieve a solution.

7.6 Summary

The Monte Carlo method plays two distinctly different roles in conduction and in radiation. In conduction, an abstraction using particles or random walks is used to simulate a solution of a partial differential equation, whereas in radiation a physical phenomenon, the transfer of photons, is simulated. The usefulness of the Monte Carlo method in thermal radiation has been fully established; it is one of the most important tools for dealing with radiation in absorbing, emitting, and scattering media. However, when dealing with the Laplace and diffusion equations, it has been used-only in practical applications where the number of coordinates in large. Since the maximum number of coordinates in thermal conduction problems is three, the need for Monte Carlo solutions has been limited. The development of new engineering materials has created numerous situations where the size and shape of the geometries may require incorporation of the Monte Carlo method with other numerical techniques to reduce the size of a problem to a manageable level.

8. AVERGAE MAGNITUDE ANALYSIS METHOD

The method of Average Magnitude Analysis is a mixture of the Integral Method and the Order of Magnitude Analysis. In this method the governing differential equations are converted to a system of algebraic equations, where the result is a sum of the order of

magnitude of each term, multiplied by a weight coefficient. These coefficients are determined from integrals containing the assumed velocity and temperature profiles. The method is used in the case of natural convection over an infinite flat plate with and without the presence of a horizontal magnetic field, and subsequently to enclosures of aspect ratios of one or higher [47]. The Average Magnitude Method (AMA) was first introduced by solving the problem of drag and heat transfer over an infinitely long flat plate. It was shown that it is equivalent to the familiar integral method.

When the problem of natural convection over an infinitely long vertical flat plate was solved, it was shown that the AMA method had an advantage of clarity and simplicity over the integral method in terms of the role and meaning of the non-dimensional numbers Ra, Bo, and Pr. The same problem was solved in the presence of a horizontal magnetic field.

Finally the AMA method was applied to the solution of the natural convection problem in enclosures and because of the complexity of the geometry and boundary conditions it was not possible to calculate the three weight coefficients. The problem was handled by carrying these coefficients as unknowns. They were subsequently determined from a mixture of theoretical, numerical, and experimental information.

9. ILLUSTRATIVE APPLICATIONS

In this paper, a few applications of the numerical methods will be illustrated. The methods have been extensively tested and applied to a variety of practical situations. A review paper (Patankar [48]) written the SIMPLE procedure contains a number of examples that were available at that time. Since, many more applications have appeared in the literature. A partial list of the published applications of the method now follows.

Two-dimensional elliptic situations involving fluid flow and heat transfer have been computed by Abdel-Wahed, Patankar, and Sparrow [49], Majumdar and Spalding [50], Patankar, Liu, and Sparrow [51], Sparrow, Patankar, and Ramadhyani [52], Patankar, Ramadhyani, and Sparrow [53], Ganesan, Spalding, and Murthly [54], Patankar, Sparrow, and Ivanovic [55], and Patankar, Ivanovic, and Sparrow [56].

Among the examples presented in this paper, a special version of the mixing-length model is employed in section (9-1). Conduction, convection, and radiation through a rectangular enclosure having cavity heated and cooled at horizontal sides while kept insulated at vertical sides as indicated in section (9-2). Finite element versus finite-difference in the case of integral and integro-differential systems through plates as indicated in section (9-3).

9.1 Turbulent Flow and Heat Transfer in Internally Finned-Tubes

A circular tube with longitudinal internal fins is considered to be an effective device for heat transfer enhancement. The fully developed flow and heat transfer in such a tube were computed by the use of a mixing-length model formulated for the cross-sectional geometry shown in Fig. (7). Complete details of the model and the resulting solutions are given in Patankar, Ivanovic, and Sparrow [56]. It is sufficient to note that the model calculates the local mixing length based on the distances of a point from both the fin surface and the tube wall, and that the turbulent viscosity is influenced by the velocity gradients in both the radial and circumferential directions. The model

incorporates a single adjustable constant, which was chosen to give good agreement with the experimental data for air flow reported by Carnavos (1977).

Figure (8) shows the comparison of the predicted values of the Nusselt number and the friction factor with experimental data. In a way, the satisfactory agreement shown is not surprising, because the adjustable constant in the model was derived from the same experimental data. On the other hand, that the adjustment of a single constant is able to give good predictions for both Nu and f over a range of Reynolds numbers and for different numbers and heights of fins is a significant achievement of the model.

9.2 Heating of a Rectangular Solid from Below

Figure (9) shows a comparison between the measured and the predicted temperatures for $\Delta T = 34\ ^{\circ}C$. The symbols denote the data points and the solid line indicate numerical predictions in the wall. The agreement between the data and predictions is excellent. This may be in part due to small temperature difference between the horizontal walls and the fact that the solid temperatures are more "forgiving" and provide less critical measure of comparison.

Figures (10) and (11) present comparisons of the measured and predicted temperatures in the cavity for $\Delta T = 52\ ^{\circ}C$ and $68\ ^{\circ}C$, respectively. The symbols denote the data points, and the solid and dashed lines represent the numerical predictions without radiation and with radiation included in the model, respectively. In the absence of radiation exchange, the model under-predicts the data at point 3 (15.8 % and 16.0 %) and 4 (8.5 % and 11 %), but over-predicts the temperature little at point 1 (2.4 % and 4.9 %) for $\Delta T = 52\ ^{\circ}C$ and $68\ ^{\circ}C$, respectively. In the presence of radiation, the model over-predicts the temperatures at points 3 (11.6 % and 7.4 %) and 4 (11.8 % and 15.3 %), but under-predicts the temperatures at point 1 (4.9 % and 1.7 %) for $\Delta T = 52\ ^{\circ}C$ and $68\ ^{\circ}C$, respectively. It should be noted that the deviation appears to be quite large at the points 3 and 4 since the error was calculated on the percentage basis, but the disagreement between the data and predictions is less than a couple of degree Celsius. It is difficult to conclude which model yields better overall agreement with the data, since the predictions of the two models agree quite well with the measurements. The model with radiation included shows better agreement at the higher modified Rayleigh number (Figure (11)).

9.3 Integral and Integro-Differential Systems

The governing equations for radiative heat transfer are of integral and/ or integro-differential systems. Integral equations arise in the process of summing the radiation intensity over the optical depths between surfaces or in enclosures, whereas integro-differential equations occur in combined mode radiation with conduction and/or convection through participating gases[57-60].

Finite-element methods are in a similar category in which differential equation are converted into integral forms[61-66].The finite-element method offers easy modeling of geometries and integration through optical depths in three dimensions as well as in the finite-element domain [67]. The finite-element equations are generated by variational methods or weighted residual methods. The variational methods require the existence of variational principle corresponding to the governing equation, whereas the weighted residual methods are independent of variational principles.

For illustration, one can choose simple geometries, as shown in Figs. (12) and (13). The results based on linear isoparametric elements and two-point Gaussian quadrature, are given in Table (5). It is shown that the most accurate results are obtained for parallel surfaces. In the case of intersecting surfaces with smaller angles, more refined grids and an additional number of Gaussian points are required for convergence (Figs. (12-14)). The reader is reminded that the power of the finite-element method is its ability to handle irregular geometries rather than a simple case, as shown in this example. If convergence is guaranteed from the basic mathematical viewpoint, the accuracy of the solution for irregular geometries can be guaranteed. The numerical results shown here are based on linear interpolation functions and a rather small number of Gaussian points (2 and 4). Although higher-order finite-element interpolation functions and/or an additional number of Gaussian points may be used for further improvement in accuracy, it has been demonstrated that such attempts are not necessary in the examples shown in the present study.

For example, consider an emitting, absorbing, and scattering medium between two infinitely large parallel plates. Solutions of this problem were presented by Viskanta [68] and Fernandes and Francis [69]. The boundary conditions are:

$$\theta = 1 \qquad \text{at } \tau = 0$$
$$\theta = T_2/T_1 = \theta_2 = 1/2 \qquad \text{at } \tau = \tau_O$$

where θ is the dimensionless temperature, τ is the optical depth.

The results of the Galerkin finite-element solution of are given in Fig. (15) (N =1, where N is the ratio of radiation over convection) for temperature distributions (N = 1) and in Table (6) (N = 1) and Table (7) (N = 10) for temperature gradient and heat fluxes. A total of 20 one-dimensional elements are used in this analysis. The dimensionless radiative heat flux Ψ is calculated from the expression

$$\Psi = -4N\frac{d\theta}{d\tau} + \hat{\Psi} \qquad (20)$$

Note that the increase in the albedo ω_o for single scattering results in a decrease of temperature and the radiation function (Fig. (15)). A similar trend exists for the temperature gradients and heat fluxes (Tables (6) and (7)). It is seen that the heat flux increases with an increase in emissivity, whereas the temperature gradients are slightly decreased when emissivity is increased. The finite-element results are in good agreement with Viskanta [68] and with Fernandes and Francis [69].

The results obtained using 20 linear elements are compared in Table (8) and Fig. (16). Here, the effects of N and the optical thickness τ_o on temperature gradients, radiation heat flux, the total heat flux, and the Nusselt number $[Nu = 2\tau_o\Psi/4N(1-\theta_b)]$ are shown. It is noted that for a large value of N (less convection and radiation dominating), the agreement is close; for a small value of N (more convection and radiation dominating) and for a large optical thickness, however, we seem to have poor agreement compared with Viskanta [70], who used Taylor series expansions for the variables.

Table 5. View factors F_{A-B} for two square planes, Two-Point Gaussian Quadrature.

Solution Schemes		Two Parallel Planes	Geometries: Two Intersecting Planes 30°	60°	90°	120°	150°
Analytic solution		0.19983	0.62020	0.37120	0.20004	0.08700	0.021510
Finite Elements	3 × 3	0.19980	1.53905	0.51115	0.23359	0.09541	0.02299
			1.09247[a]	0.45421[a]			
	5 × 5	0.19982	1.17043	0.45474	0.22015	0.09196	0.02236
	8 × 8	0.19982	0.96347	0.42319	0.21261	0.08998	0.02199
			0.79660[a]	0.40214[a]			
	20 × 20	—	0.75673	0.39177	0.20506	0.08797	0.02160
	30 × 30	—	0.71082	0.38481	0.20339	0.08751	0.02152
	40 × 40	—	0.68786	0.38133	0.20255	0.08729	0.02147

[a]Results for six-point Gaussian quadrature

TABLE 6. Combined Conduction-Radiation Heat Transfer, Effect of Emissivity for $N = 1$, $\theta = 1$, $\theta_2 = \frac{1}{2}$, $\tau_0 = 1$, on Temperature Gradients and Heat Flux

		$\left.\frac{d\theta}{d\tau}\right\|_{\tau=0}$			$\hat{\Psi}(0)$			Ψ		
ω_0	$\varepsilon_1 = \varepsilon_2$	[68]	[69]	[25]	[68]	[69]	[25]	[68]	[69]	[25]
0.0	1.0	−0.5019	−0.5020	−0.498	0.5656	0.5650	0.5650	0.6433	0.6430	0.6400
	0.5	−0.5240	−0.5240	−0.5170	0.2676	0.2670	0.2670	0.5909	0.5900	0.5840
	0.1	−0.5410	−0.5430	−0.5340	0.0514	0.0520	0.0510	0.5538	0.5560	0.5470
0.5	1.0	−0.4967	−0.4960	−0.4950	0.5626	0.5630	0.5640	0.6374	0.6370	0.6360
	0.5	−0.5109	−0.5100	−0.5070	0.2733	0.2730	0.2730	0.5792	0.5790	0.5760
	0.1	−0.5245	−0.5250	−0.5200	0.5490	0.0550	0.0550	0.5382	0.6390	0.5340
1.0	1.0	−0.5000	−0.5000	−0.5000	0.5251	0.5180	0.5250	0.6313	0.6290	0.6310
	0.5	−0.5000	−0.5000	−0.5000	0.2505	0.2450	0.2520	0.5626	0.5610	0.5630
	0.1	−0.5000	−0.5000	−0.5000	0.0525	0.0470	0.0550	0.5131	0.5120	0.5130

TABLE 7. Combined Conduction-Radiation Heat Transfer, Effect of Temperature for $N = 10$, $\tau_0 = 1$, $\theta_1 = 1$, $\varepsilon_1 = \varepsilon_2 = 1$ on Temperature Gradients and Heat Flux

		$\left.\frac{d\theta}{d\tau}\right\|_{\tau=0}$		$\hat{\psi}(0)$		ψ	
ω_0	θ_2	[68]	[25]	[68]	[25]	[68]	[25]
0.0	0.1	−0.8017	−0.7495	0.5488	0.6491	2.4237	2.3724
	0.5	−0.6415	−0.5430	0.5327	0.5381	1.9733	1.8883
0.5	0.1	−0.7592	−0.7349	0.6412	0.6430	2.3622	2.3424
	0.5	−0.5175	−0.4983	0.5428	0.5454	1.8745	1.8619
1.0	0.1	−0.9000	−0.9000	0.5553	0.5592	2.2882	2.2981
	0.5	−0.5000	−0.5000	0.5191	0.5250	1.7977	1.8126

TABLE 8. Combined Conduction-Convection-Radiation Heat Transfer without Scattering and Viscous Dissipation, $\varepsilon_1 = \varepsilon_2 = 1$, Data at the Wall

		$\left.\frac{d\theta}{d\tau}\right\|_{\tau=0}$		$\hat{\psi}(0)$		ψ		Nusselt Number	
τ_0	N	[70]	FEM	[70]	FEM	[70]	FEM	[70]	FEM
0.1	10.0	−14.290	−14.327	0.1164	0.1152	571.716	573.360	7.542	7.561
	0.1	−14.230	−14.500	0.1164	0.1156	5.808	5.912	7.668	7.788
1.0	10.0	−1.4246	−1.4876	0.5112	0.5128	57.496	60.018	7.589	7.878
	0.1	−1.1991	−1.4965	0.4880	0.5132	0.978	1.111	13.352	14.582

[a]Due to different definitions and signs for $\hat{\psi}$ and ψ in [70] the Viskanta results are multiplied by 4.

9.3.1 Concluding Remarks

The subject of integral and integro-differential system as a branch of applied mathematics and as a method that can be used for practical applications in radiative heat transfer has been discussed with solution techniques based on finite-element theory.

Simple examples of the Fredholm and Volterra equations are demonstrated, followed by increasingly complicated radiative heat transfer problems. With only linear finite-element interpolation functions, a high degree of accuracy was obtained for the selected example problems having exact solutions. It was also shown that with Galerkin finite elements the solution procedure is simple, systematically general, and robust for all types of integral and/or integro-differential equations, with step-by step solution strategies being independent of the problem at hand. Gaussian quadrature integration schemes for both the optical depth and finite-element spaces play decisive roles in the success of finite-element approaches.

Difficulties resulting from the terms due to convection, however, persist, if combined-mode radiative heat transfer is considered. Convergence to the true solution is difficult to achieve as convection becomes dominant because of the ill-conditioning of the convection finite-element matrices. Such ill-conditioning stems from the linearly dependent system of equations or the nearly singular matrix when the flow field is highly rotational or convective. To overcome these difficulties, mesh refinement and/or higher-order interpolation functions are required, with a corresponding substantial increase in computational time and storage. From the point of view of linear algebra, the mesh refinement serves to strengthen the diagonal and weaken the off-diagonal terms, shifting the matrix toward a linearly independent or strongly nonsingular system of equations. Current research in this vein include an adaptive mesh program that is believed to be the key to the success for all ill-conditioned equation systems. [25]

If convection is less dominant, however, the solution of integral and integro-differential systems does not present any significant problems. For these situations, the finite-element theory provides a very general and robust methodology, independent of arbitrary and complicated geometries and boundary conditions.

NOMENCLATURE

Symbol	Definition
AR	Aspect ratio of the cavty
BO	Boussinesq number
C	Courant number, $= u\Delta t / \Delta x$
C_p	specific heat
D	Diffusivity
F	view factor
f	friction factor
F	Fourier number
g	amplification function
G	amplification factor
h	convective heat transfer coefficient
H	height of the fins through tube
H	height of the enclosure
i	node location
k	thermal conductivity
k*	thermal conductivity ratio
L( )	differential operator
n	outward unit vector
N	No. of fins
Nu	Nusselt number
p	variable in Barakat and Clark method
Pr	Prandtl number
q	variable in Barakat and Clark method
r_o	radius of the tube
R	residual, =L(ϕ)-f
Ra	Rayleigh number
Ra*	modified rayleigh number
T	temperature
t	time
u	horizontal velocity
U	constant horizontal velocity
v	laterial velocity
V	velocity vector
w	vertical velocity
W	weighting function
x	horizontal coordinate
$\bar{x}$	multidimensional
y	lateral coordinate
z	vertical coordinate

Greek Symbols

$\propto$	thermal diffusivity
$\propto^*$	thermal diffusivity ratio
Δt	time interval
Δ_o	central-difference operator
δ^2	second derivative operator
$\delta^2\Delta_{\pm}$	third(upwind) derivative operator
θ	weighting factor
θh, θc	dimensionless temperature
λ	$\Delta t / \Delta x^2$
τ	optical distance
Λ	angular frequency, $=\Omega + i\upsilon (i = \sqrt{-1})$
υ	kinamatic viscosity
ξ_1, ξ_2	random variables
ξ	two-dimensional natural coordinates
η	random variable
ϕ	transport variable
ϕ'	void fraction
β	angle of intersection plans
ω_o	albedo
ε	deformation factor

Subscripts

i+1, i, i-1	node locations
j, k,l	node locations
num	numerical
t	$=\partial / \partial t$
x	$=\partial / \partial x$
H	heating
C	cooling

Superscripts

n	present time
n+1	new time

Mathematical Symbols

∇	$i\frac{\partial}{\partial x} + j\frac{\partial}{\partial y} + k\frac{\partial}{\partial z}$

REFERENCES

1. G. F. Pinder and W. G. Gray, Finite Element Simulation in Surface and Subsurface Hydrology, Academic Press, New York,1977
2. L. F. Richardson, "The approximate Arithmetical Solution by Finite Difference of Physical Problems Involving Differential Equations, with an Application to the Stresses in a Masonry Dam," Phil. Trans. Roy. Soc. London, Ser. A, 210, 307-357, 1910.
3. D. A. Anderson, J. C. Tannehill, and R. H. Pletcher, "Computational Fluid Mechanics and Heat Transfer," Hemisphere, New York, 1984.
4. J. Crank and P. Nicolson, "A Practical Method for Numerical Evaluation of Solutions of Partial Differential Equations of the Heat-Conduction Type," Proc. Combridge Phil. Soc., 43, 50-67, 1947.
5. E. C. DuFort and S. P. Frankel, "Stability Conditions in The Numerical Treatment of Parabolic Differential Equations," Mathematical Tables and Other Aids to Computation, Vol. 7, 1953, pp. 135-152.
6. H. Z. Barakat and J. A. Clark, "On the Solution of the Diffusion Equations by Numerical Methods," J. Heat Transfer, 87-88, 421-427, 1966.
7. D. W. Peaceman and H. H. Rachford, "The Numerical Solution of Parabolic and Elliptic Differential Equations," J. Soc. Ind. Appl. Math., 3, 28-41, 1955.
8. J. Douglas, Jr., "On the Numerical Integration of $\partial^2 u/\partial x^2 + \partial^2 u/\partial y^2 = \partial u/\partial t$ by Implicit Methods," J. Soc. Ind. Appl. Math., 3, 42-65, 1955.
9. J. Douglas and J. E. Gunn, "A General Formulation of Alternating Direction Methods-Part I. Parabolic Problems," Numerische Mathematik, 6, 428-453, 1964.
10. D. Kim, "Heat Transfer by Combined Conduction, Convection, and Radiation Through a Solid with a Cavity," Ph. D. Thesis, Purdue University, Indians, 1983.
11. P. J. Roache, "Computational Fluid Dynamics," Hermosa, Albuquerque, New Mexico, 1972.
12. D. R. Chenoweth, D. R., and Paolucci S., "On Optimizing Non-Uniform Finite Difference Grids for Boundary Regions in Transient Transport Problems," Report SAND 81-8204, Sandia, National Laboratories, Livermore California.
13. K. Küblbeck, M. P. Merker and J. Straub, "Advanced Numerical Computation of Two-Dimensional Time-Dependent Free Convection in Cavities, Int. J. Heat Mass Transfer, Vol. 23, pp. 203-217, 1980.
14. M. Holt, Numerical Methods in Fluids Dynamics, Springer, Verlag, New York ,1977.
15. A. J. Baker, Finite Element Computational Fluid Mechanics, McGraw-Hill/Hemisphere, New York, 1983.

16. T. J. R. Hughes , W. T. Liu, and A. Brooks ,"finite Element Analysis of Incompressible viscous Flows by the Penalty Function Formuation,", J. Comput Phys. , 30,1-60,1979.

17. R. Peyret and T.D. Tayler, Computational Methods for Fluid Flow , Springer-verlag. New York, 1983.

18. D. Gottlieb and S. A. Orszag, Numerical Analysis of Spectral Methods, SIAM, Philadelphia, PA,1977

19. T. J. Rivlin, the Chebyshev Polynomials, Wiley-Interscience, New York,1974

20. L. Fox and T. B. Parker, Chebyshev Polynomials in Numerical Analysis, Oxford Press, London, 1968

21. T. J. Chung, "Finite Element Analysis in Fluid Dynamics," McGraw-Hill, New York, 1978.

22. J. M. Ortega and W. C. Rheinboldt, "Iterative Solution of Nonlinear Equations in Several Variables," Academic Press, New York, 1970.

23. B. Cathers and B. A. O'Connors," The Group velocity of Some Numerical Schemws," Int. J. Numer. Methods Fluids, 5, 201-224,1985.

24. B. A. Finlayson, " Non-linear Analysis in Chemical Engineering," McGraw-Hill, New York, 1980.

25. W. J. Minkwycz, E. M. Sparrow, G. E. Schneider, and R. H. Pletcher, "Hand-Book of Numerical Heat Transfer," John Wiley and Sons, 1988.

26. B. Canahan, M. A. Luther, and J. O. Wilkes, "Applied Numerical Methods, Wiley, New York, 1969.

27. P. Li and C. J. Chen, "The Finite Differential Method-A Numerical Solution to Differential Equations," Proceedings, 7th Canadian Congress of Applied Mechanics, Sherbrokke, May 27-June 1, 1979.

28. C. J. Chen, M. Z. Sheikholeslami, and R. B. Bhiladvala, "Finite Analytical Numerical Method for Linear and Nonlinear Ordinary Differential Equations," 8th International Conference on Computing Method in Applied Science and Engineering, Versailles, France, Dec. 14-18, 1987. Also J. Computer Meth. in Applied Mechanics and Engineering, Vol. 40, 1988.

29. C. J. Chen and V. Talaie, "Finite Analytic Numerical Solutions of Laminar Natural Convection in Two-Dimensional Inclined Rectangular Enclosures," 1985 National Heat Transfer Conf., Denver, CO, Aug. 4-7, 1985, ASME paper 85-HT-10.

30. V. Talaie and C. J. Chen, "Finite Analytic Solution of Steady and Transient Natural Convection in Two-Dimensional Rectangular Enclosures," presented at 1985 ASME Winter Annual Meeting, Miami, FL, Nov. 17-22, 1985, ASME paper 85-WA/HT-68.

31. C. J. Chen and Y. H. Yoon, "Prediction of Turbulent Heat Transfer in Flow Past a Cylindrical Cavity," presented at 1985 Winter Annual Meeting, Symposium on

Mixed Convective Heat Transfer, Miami, FL, Nov. 17-22, 1985, ASME 85-HTD, Vol. 53, ED. by B. F. Armaly and L. S. Yao, pp. 1-8

32. C. J. Chen and S. M. Chang, "Prediction of Turbulent Flows in Rectangular Cavity with k-ε-A and k-ε-E Models," presented at 2nd International Symposium on Refined Flow Modeling and Turbulent Measurements, Iowa City, IA, Sept. 16-18, 1985, also in Hemisphere Pub. Corp., 1987, pp. 611-620.

33. C. J. Chen, C. H. Yu, and K. B. Chandran, "Finite Analytic Numerical Solution of Unsteady Laminar Flow Past Disc-Valves," J. Engineering Mechanics, Vol. 113, No. 8, Aug. 1987, pp. 1147-1162.

34. C. J. Chen, C. H. Yu, and K. B. Chandran, "Steady Turbulent Flow Through a Disc-Type Valve-I: Finite Analytic Solution," J. Engineering Mechanics, Vol. 114, 1988.

35. C. H. Yu, C. J. Chen, and K. B. Chandran, "Steady Turbulent Flow Through a Disc-Type Valve-II: Parametric Study on Disc Size and Position," J. Engineering Mechanics, Vol. 114, 1988.

36. Y. N. Xu and C. J. Chen "Finite Analytic Numerical Prediction of Flow Over Flat Plate and Near Wake," Proc. 20th Midwestern Mechanics Conference, West Lafayette, IN, Aug. 31-Sept. 2, 1987, pp.519-524.

37. V. C. Patel and H. C. Chen, "Turbulent Wake of A Flat Plate," J. AIAA, Vol. 25, No. 8, 1987, pp. 1075-1085.

38. C. J. Chen and W. C. Chen, "Prediction of Supersonic Oblique Shock Wave in Arbitrary Internal Passage by Methods of Characteristics," Numerical Methods in Laminar and Turbulent Flow, Vol. 5, 1987, pp. 1009-1020.

39. K. Binder, "Applications of the Monte Carlo Method in Statistical Physics," Springer-Verlag, Berlin, 1984.

40. H. Kahn, "Application of Monte Carlo," U. S. Atomic Energy Commission Report, Rand Corp., No. AECU-3259,1956.

41. I. M. Sobol, "The Monte Carlo Method," University of Chicago Press, 1974, (English translation).

42. G. E. Zinsmeister and S. S. Pan, "A Modification of the Monte Carlo Method For Steady Heat Conduction Problems," Int. J. Numer. Methods Eng., 10, 1057-1064, 1976.

43. J. R. Howell and M. Perlmutter, "Monte Carlo Solution of Thermal Transfer Through Radiant Media Between Gray Walls," J. Heat Transfer, 86 (1), 116-122, 1964.

44. M. Perlmutter and J. R. Howell, "Radiant Heat Transfer Through a Gray Gas Between Concentric Cylinders Using Monte Carlo," J. Heat Transfer, 86, (2), 169-179, 1964.

45. L. C. Polgar and J. R. Howell, "Directional Thermal-Radiative Properties of Conical Cavities," NASA TN D-2904,1965.

46. J. R. Howell, "Application of Monte Carlo to Heat Transfer Problems," Adv. Heat Transfer, 5, 1-54; 1968.

47. P. S. Lykoudis, "Introduction to the Method of Average Magnitude Analysis and Application to Natural Convection, ASME, J. of Heat Transfer, Vol. 117, Aug. 1995.

48. Patankar S. V., Rafiinejad D., and Spalding D. B., "Calculation of the Three-Dimensional Boundary Layer With Solutions of All Three Momentum Equations Comp," Methods Appl. Mech. Eng. Vol. 6, p.283, 1975.

49. Abdel-Wahed, R. M., Patankar, S. V., and Sparrow, E. M., "Fully Developed Laminar Flow and Heat Transfer in a Square Duct With One Moving Wall," Lett. Heat Mass Transfer, Vol. 3, p. 355, 1976.

50. Majumdar, A. K. and Spalding, D. B., "Numerical Computation of Taylor Vortices," J. Fluid Mech., Vol. 81, p. 295, 1977.

51. Patankar, S. V., Liu, C. H., and Sparrow, E. M., "Fully Developed Flow and Heat Transfer in Ducts Having Streamwise-Periodic Variations of Cross-Sectional Area," J. Heat Transfer, Vol. 99, p. 180, 1977.

52. Sparrow, E. M., Patankar, S. V., and Ramadhyani, S., "Analysis of Melting in the Presence of Natural Convection in the Melt Region," J. Heat Transfer, Vol. 99, p. 520, 1977.

53. Patankar, S. V., Ramadhyani, S., and Sparrow, E. M., "Effect of Circumferentially Nonuniform Heating in Laminar Combined Convection in a Horizontal Tube," J. Heat Transfer, Vol. 100, p. 63. (Also see the Erratum in J. Heat Transfer, Vol. 100, p. 367, 1978.

54. Ganesan, V., Spalding, D. B., and Murthy, B. S., "Experimental and Theoretical Investigation of Flow Behind an Axi-Symmetrical Baffle in a Circular Duct," J. Inst. Fuel, Vol. 51, p. 144, 1978.

55. Patankar, S. V., Sparrow, E. M., and Ivanovic, M., "Thermal Interactions Among the Confining Walls of a Turbulent Recirculating Flow," Int. J. Heat Mass Transfer, Vol. 21, P. 269, 1978.

56. Patankar, S. V., Ivanovic, M., and Sparrow, E. M., "Analysis of Turbulent Flow and Heat Transfer in Internally Finned Tubes and Annuli," J. Heat Transfer, Vol. 101, p. 29, 1979.

57. Chandraskhar, Radiative transfer, Dover, New York, 1960

58. E. M. Sparrow and R. D. Cess, radiation Heat transfer, Brooks/Code, 1970

59. R. Siegel and J. R. Howell, Thermal radiation Heat Transfer, McGrow-Hill, New York, 1972

60. M. N. Ozisik, Radiative Transfer, Wiley-Interscience, New York, 1973.

61. T. J. Chung, Finite Element analysis in Fluid Dynamic, McGraw-Hill, New York,1978.

62. J. N. Reddy and V. D. Murty, "finite Element Solution of Integral Equations Arising in Radiative Heat Transfer and Laminar Boundary Layer Theory," Numer. Heat Transfer, 1, 389-401,1978.

63. R. Fernandes and J. Francis, " Combined Conductive and Radiative Heat transfer in an Absorbing, Emitting and Scattering Cylindrical Medium," ASME J. Heat transfer, 104, 594-601, 1982.

64. T. J. Chung, and J.Y. Kim " Radiation View Factors by Finite Elements," ASME J. Heat Transfer, 104, 792-795, 1982

65. M. L. Nice, numerical Properties Methodologies in Heat Transfer, Hemisphere, 1983, pp.497-514

66. T. J. Chung, and J.Y. Kim " Two-Dimensional Combined Mode Heat Transfer By Conduction, Convection and Radiation in Emitting, Absorbing and Scattering Media-Solution by Finite Elements, " ASME J. Heat Transfer, 106, 448-452, 1984.

67. T. J. Chung and J. Y. Kim, "Two-Dimensional Combined Mode Heat Transfer by Conduction, Convection, and Radiation in Emitting, Absorbing and Scattering Media-Solution by Finite-Elements," ASME J. Heat Transfer, 106, 448-452, 1984.

68. R. Viskanta, " Heat Transfer by Conduction and Radiation in Absorbing and Scattering Materials," ASME J. Heat Transfer, 87(1), 143-150, 1965.

69. R. Fernandes and J. Francis, "Combined Conductive and Radiative Heat Transfer in an Absorbing, Emitting, and Scattering Cylindrical Medium," ASME J. Heat Transfer, 104, 594-601, 1982.

70. R. Viskanta, "Interacting of Heat Transfer by Conduction, Convection, and Radiation in a radiating Fluid", J. Heat Transfer, 85, 318-329, 1963.

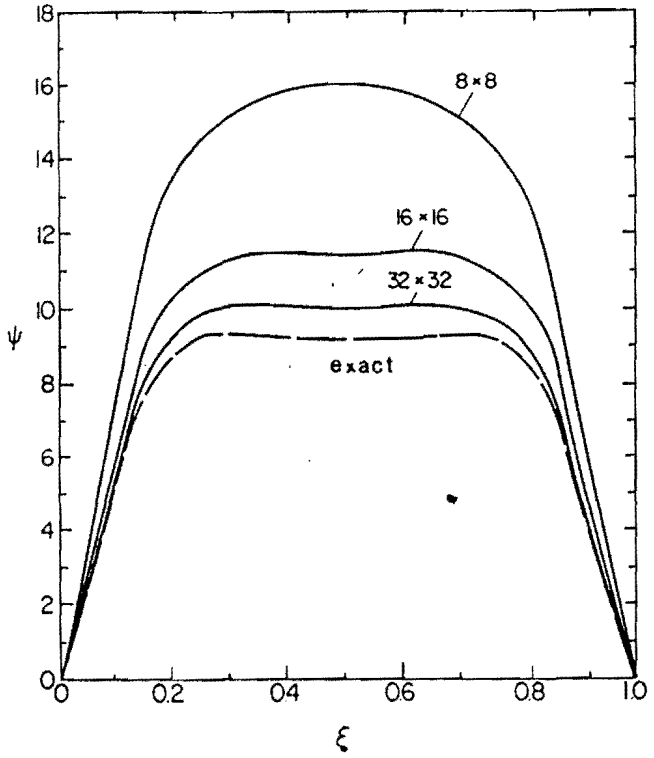

Figure 1. Effect of grid spacing on stream functions Ra = 10^5 and Pr = 0.71.

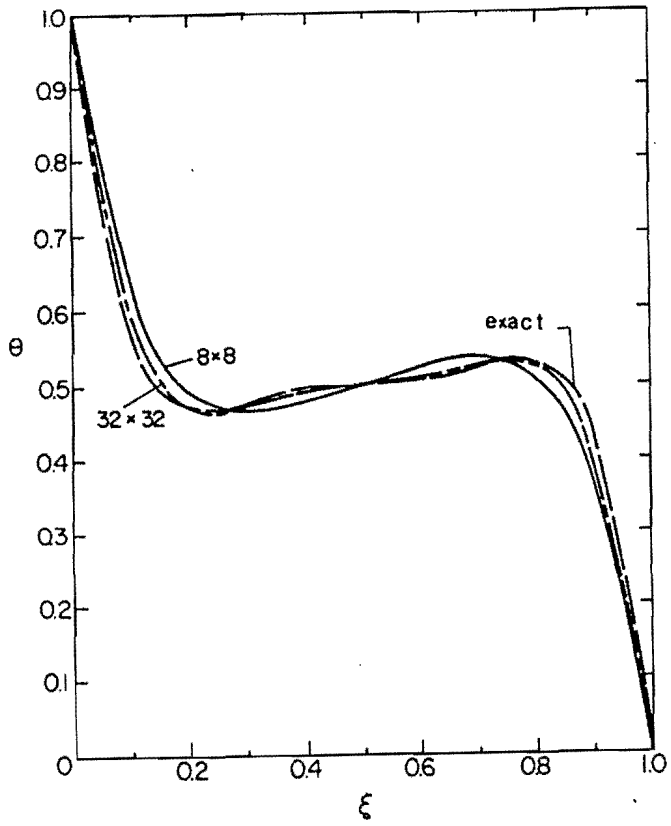

Figure 2. Effect of grid spacing on temperature distribution; Ra = 10^5 and Pr = 0.71.

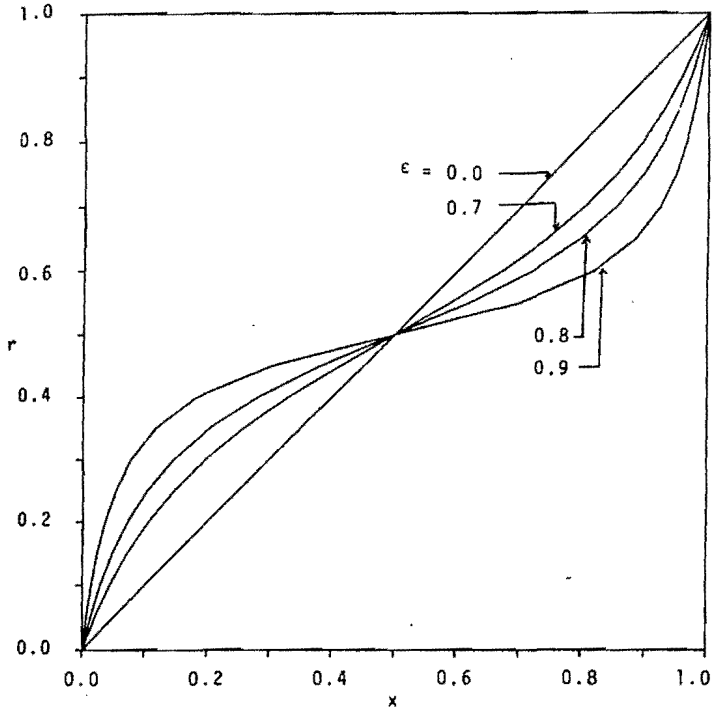

Figure 3. Transformation relation between r and x (Eq. 10).

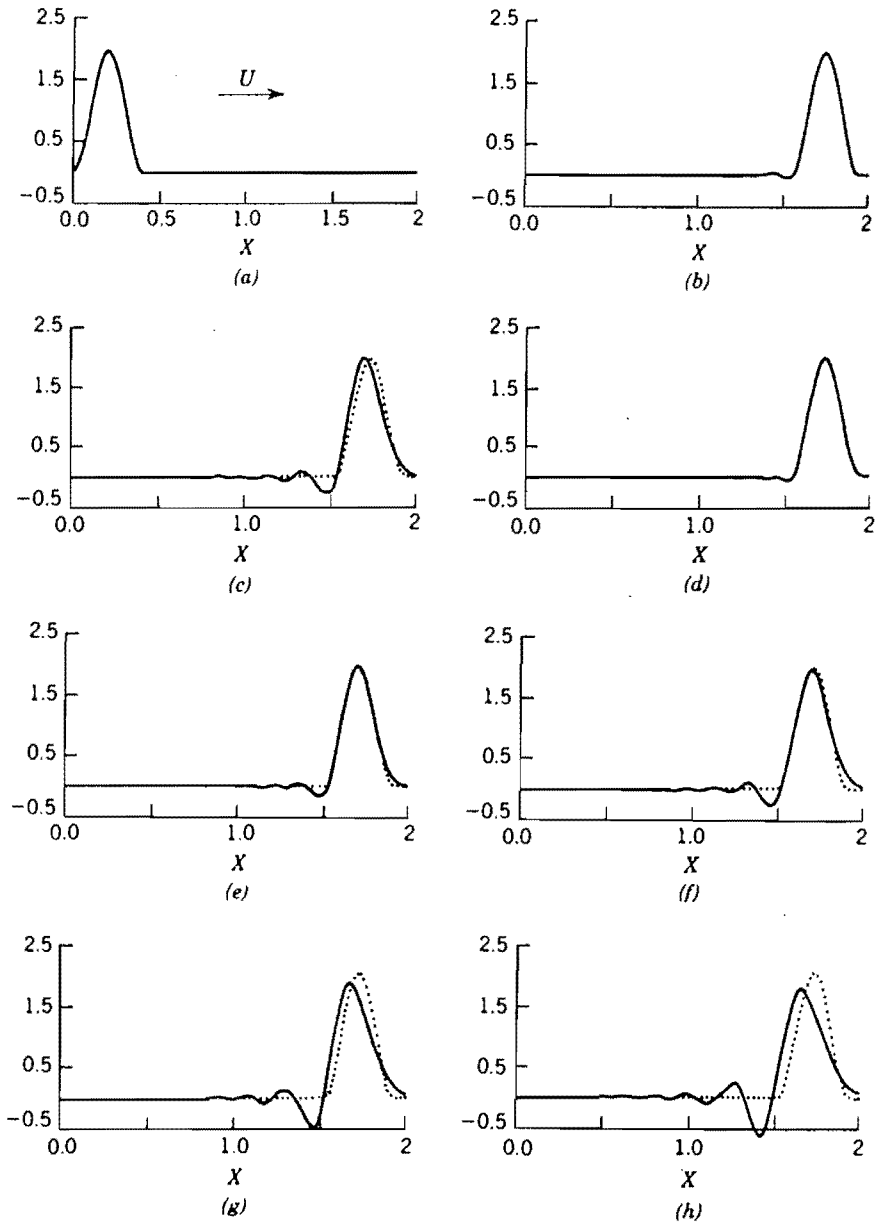

Figure 4. One-dimensional advection of a scalar distribution. (a) Initial distribution; (b) linear FEM, C=0.4; (c) Crank-Nicolson FDM, C=0.4; (d) quadratic FEM, C=0.4;(e) linear FEM, C=0.8; (f) linear FEM, C=1.2; (g) linear FEM, C=1.6; (h) Cran-Nicolson FDM, C=1.6. Exact solution denoted by dotted line ($C = U\Delta t / \Delta x$ = constant velocity)

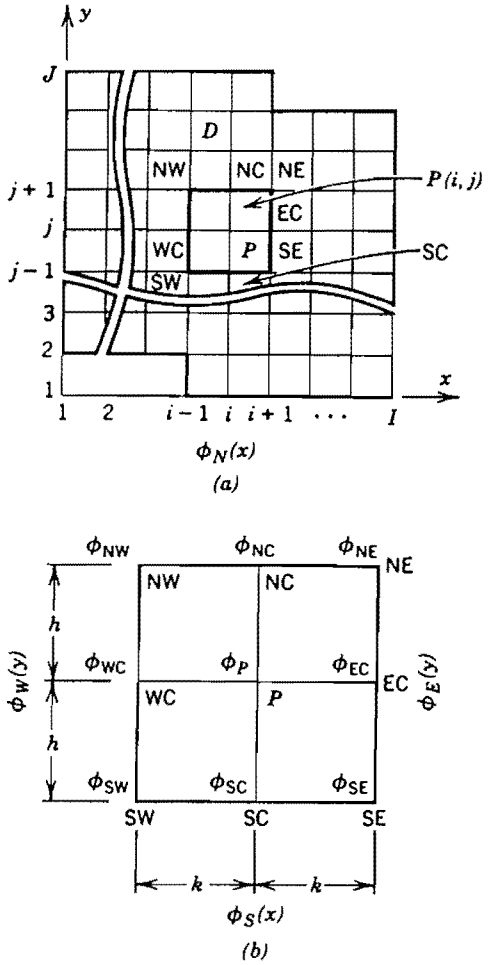

Figure 5. (*a*) Domain and (*b*) subregion of the finite analytic method.

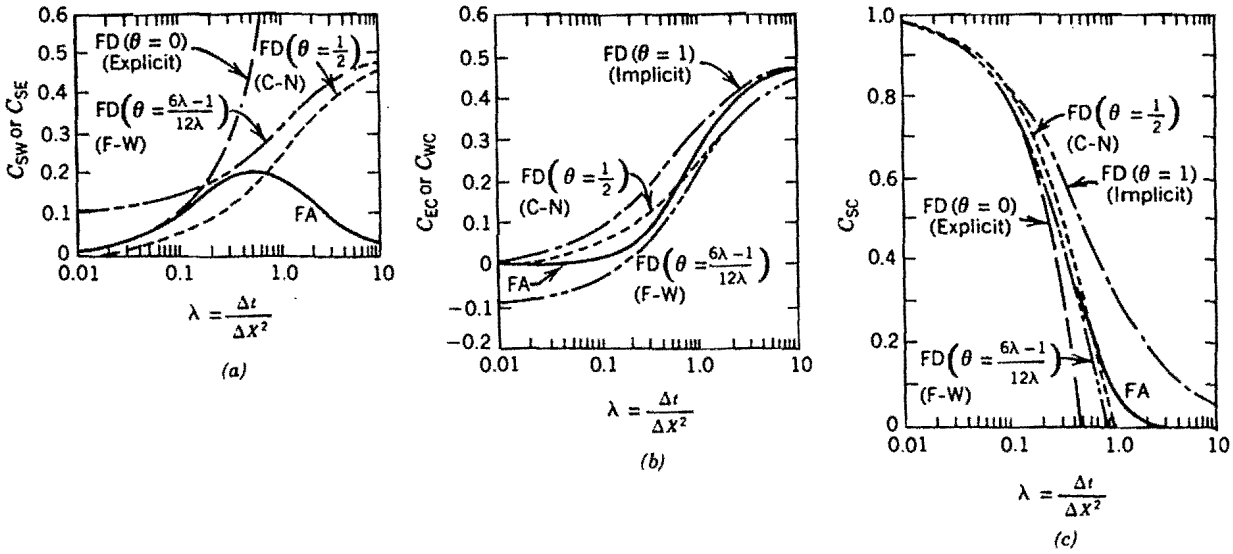

Figure 6. Comparison of finite analytic and finite-difference coefficients for heat equation. (*a*) Coefficients C_{SW} and C_{SE} vs. λ. (*b*) Coefficients C_W and C_E vs. λ. (*c*) Coefficients C_{SC} vs. λ.

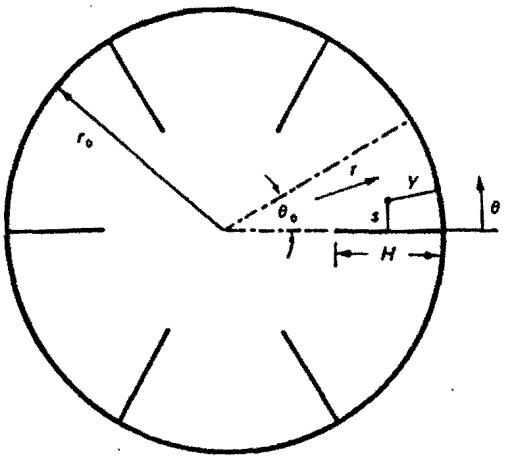

Figure 7. Cross-sectional geometry of an internally finned tube [from Patankar, Ivanovic, and Sparrow (1979)].

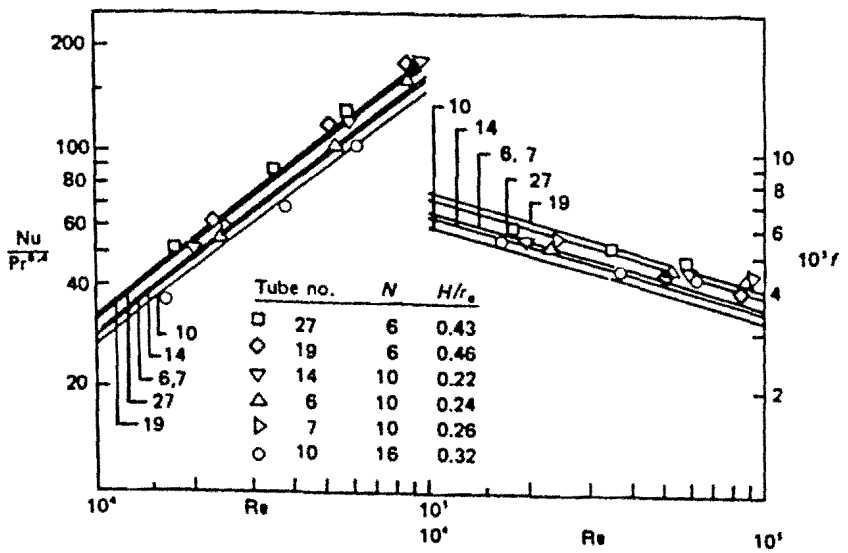

Figure 8. Comparison of predicted values of the Nusselt number and friction factor with the experimental data of Carnvos (1977) [from Patankar, Ivanovic, and Sparrow (1979)]

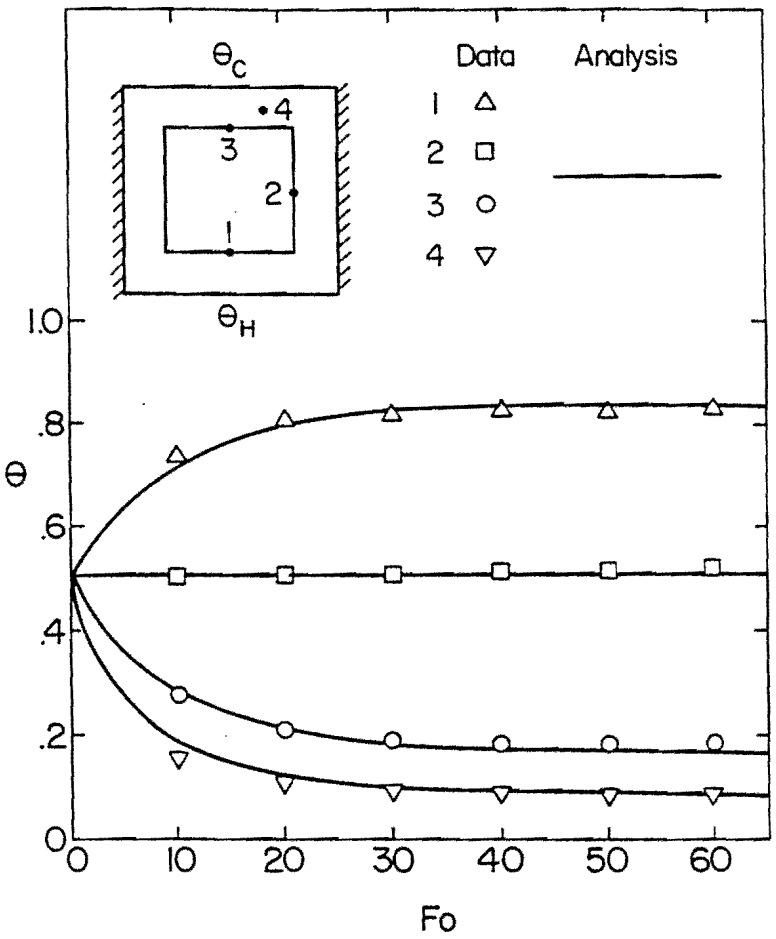

Figure 9. Comparison between the measured and predicted temperature in the walls; $Ra^* = 0.64 \times 10^6$, Pr = 0.71, AR = 1, H/L = 1.0, ϕ = 0.36, k^* = 7.4, and α^* = 0.008.

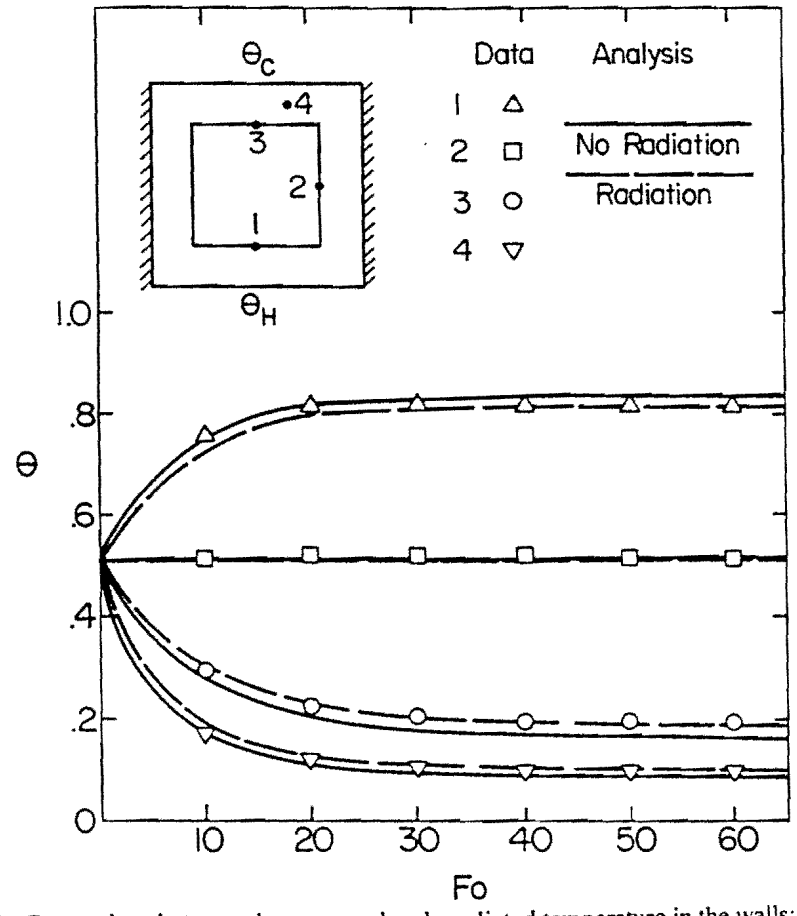

Figure 10. Comparison between the measured and predicted temperature in the walls; $Ra^* = 1.01 \times 10^6$, Pr = 0.71, AR = 1, H/L = 1.0, ϕ = 0.36, k^* = 7.4, and α^* = 0.008.

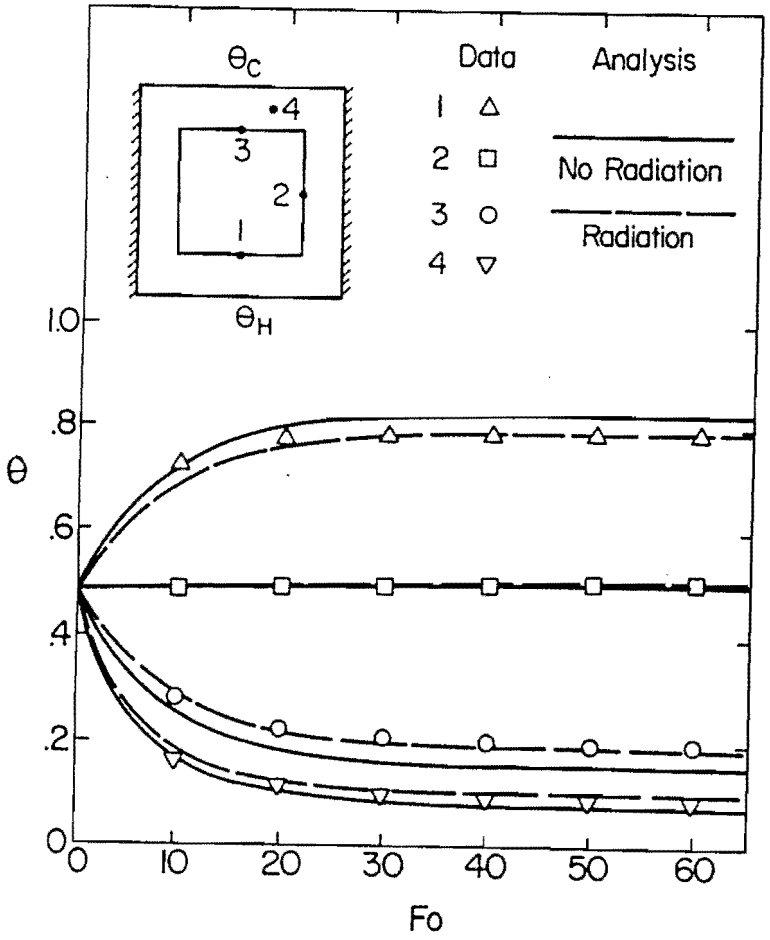

Figure 11. Comparison between the measured and predicted temperature in the walls; $Ra^* = 1.28 \times 10^6$, Pr = 0.71, AR = 1, H/L = 1.0, $\phi = 0.36$, $k^* = 7.4$, and $\alpha^* = 0.008$.

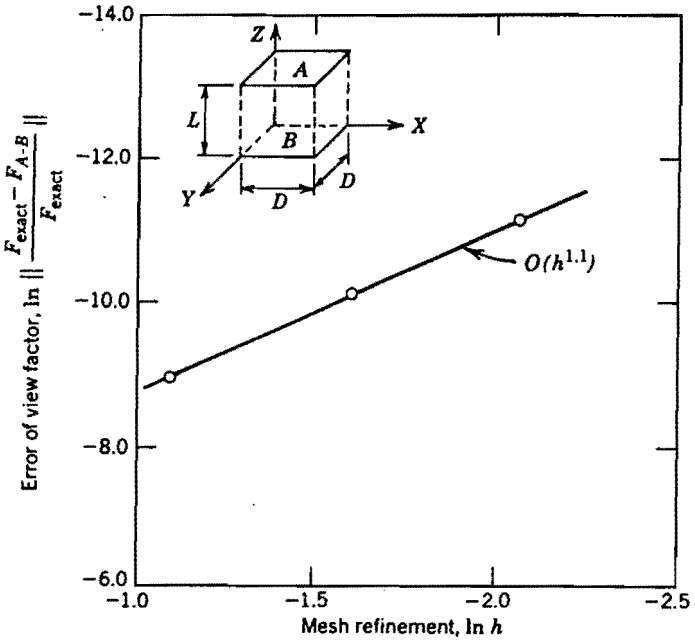

Figure 12. Convergence curve of view factor error versus mesh size for two parallel 1 × 1 square planes. One unit a part.

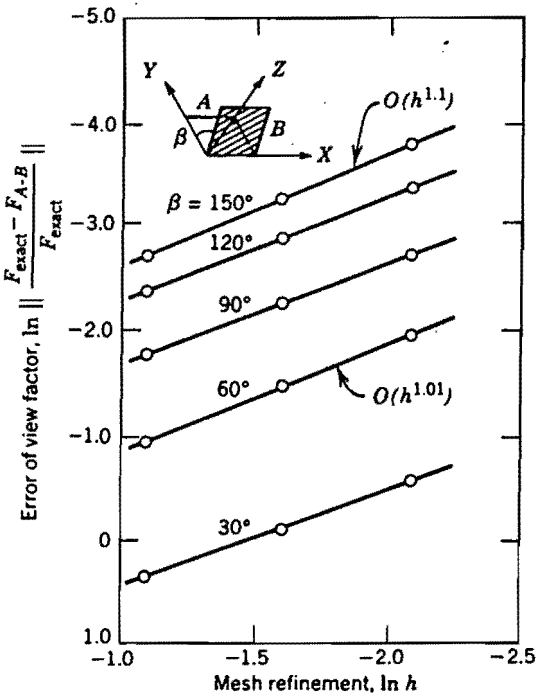

Figure 13. Convergence curves of view factor error versus mesh size for two intersecting 1 × 1 square planes at angle of 30°, 60°, 90°, 120°, and 150°

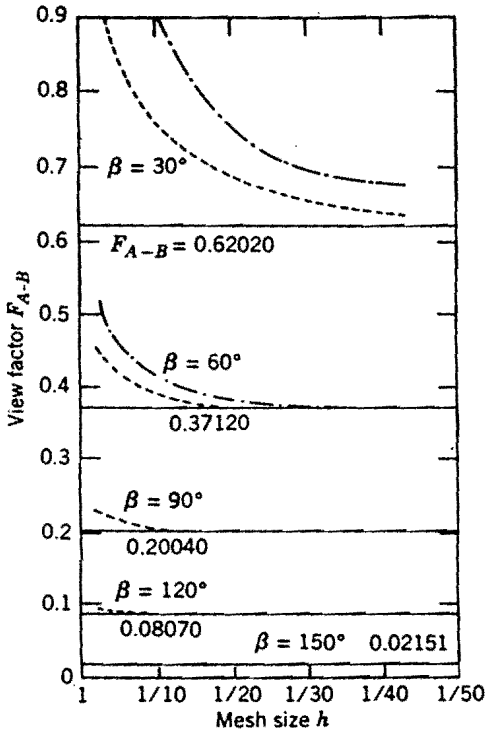

Figure 14. View factors versus mesh size for two intersecting planes. (—) Exact solution; (-.-.-.) two points Gaussian quadrature; (-----) six points Gaussian quadrature.

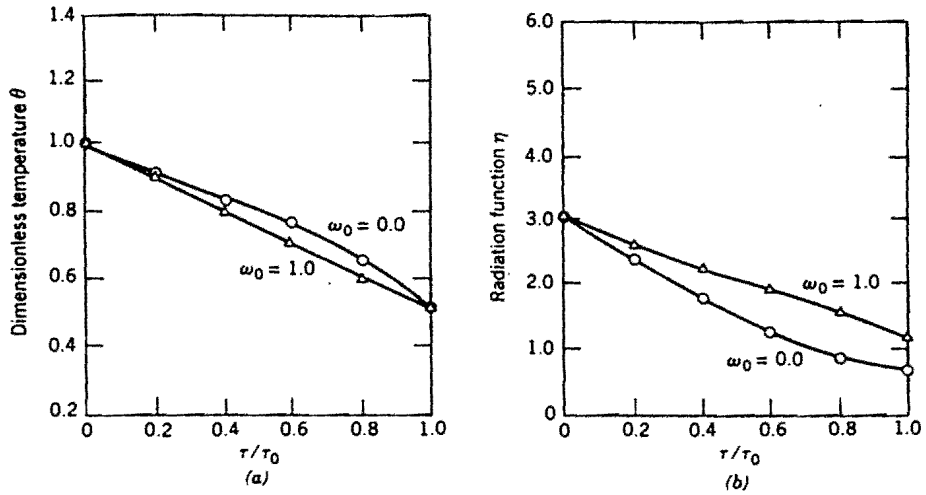

Figure 15. Combined conduction-radiation heat transfer, effects of ω_0 on the temperature and radiation function for $N = 1$, $\tau_0 = \varepsilon_1 = \varepsilon_2 = 1.0$. Symbols, finite elements; curves, Viskanta, Ref. 68.

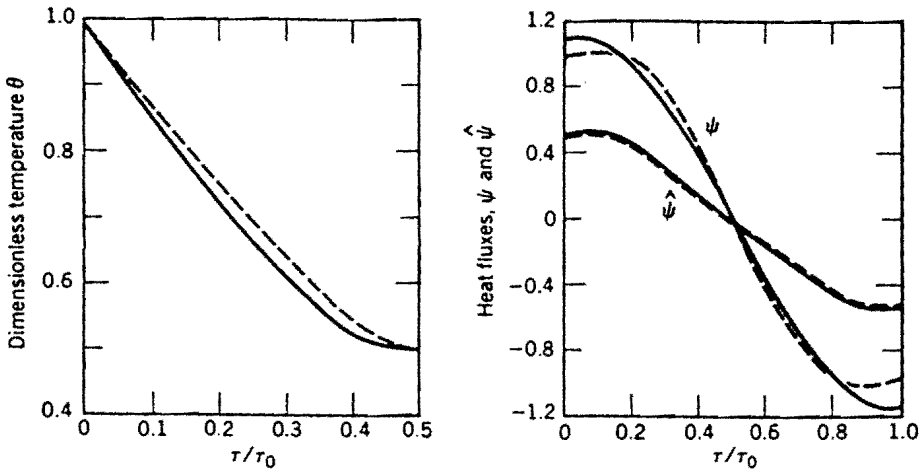

Figure 16 Combined conduction-convection-radiation heat transfer without scattering and viscous dissipation. $N = 0.1$; $\omega_0 = 0$; Ec Pr = 0; $\tau_0 = \varepsilon_1 = \varepsilon_2 = 1$.